Palaeontologia Electronica
palaeo-electronica.org

Chewing cycle analysis of *Lesmesodon edingeri* (Mammalia; Hyaenodonta) and implications for carnivoran feeding adaptions

Jannik Weidtke, Julia A. Schultz, Michael Morlo, Andreas J. Lang, Thomas Lehmann, and Thomas Martin

ABSTRACT

The dentition of the proviverrine hyaenodont *Lesmesodon edingeri* from Messel is known only from preservation in full occlusion. Moreover, only subadult individuals have been recovered so far. The µCT-based study provides new details from lingual, buccal, and occlusal aspects of its dentition, indicating new insights on the ecology of *Lesmesodon* and its niche occupation in the Messel ecosystem and what dietary range it had. We analyzed the dental function of the Eocene species *Lesmesodon edingeri* and its close relative *Proviverra typica* by reconstructing the wear facets and their respective chewing cycle with the Occlusal Fingerprint Analyser (OFA) software and compared them with those of three modern carnivorous taxa. The teeth were compared by quantification of their contact areas (wear facets) and the calculation of the duration of the contact. Subsequently the masticatory path was reconstructed in detail. Differences in morphologically similar dentitions are revealed by the OFA analysis. The insectivorous species show similarities in their respective chewing cycle in terms of duration and maximum intercuspation, while species more specialized in either carnivory or omnivory show contrary trends, that can be clearly separated from the insectivores. Our study showed that the small hyaenodont *Lesmesodon edingeri* apparently occupied a primarily insectivorous-carnivorous dietary niche in the Messel ecosystem and how the dentitions of the insectivorous species in this study differ despite having adaptions that look similar at first glance.

Jannik Weidtke. Department Palaeontology and Evolutionary Research, State Museum of National History Karlsruhe, 76133 Karlsruhe, Germany. weidtkejannik@gmail.com
Julia A. Schultz. Section Palaeontology, Bonn Institute of Organismic Biology, Rheinische Friedrich-Wilhelms-Universität Bonn, 53115 Bonn, Germany. jaschultz@uni-bonn.de
Michael Morlo. Department Messel Research and Mammalogy, Senckenberg Research Institute and Natural History Museum, 60325 Frankfurt, Germany. michael.morlo@senckenberg.de
Andreas J. Lang. Section Palaeontology, Bonn Institute of Organismic Biology, Rheinische Friedrich-

Final citation: Weidtke, Jannik, Schultz, Julia A., Morlo, Michael, Lang, Andreas J., Lehmann, Thomas, and Martin, Thomas. 2025. Chewing cycle analysis of *Lesmesodon edingeri* (Mammalia; Hyaenodonta) and implications for carnivoran feeding adaptions. Palaeontologia Electronica, 28(3):a45.
https://doi.org/10.26879/18
palaeo-electronica.org/content/2025/5643-chewing-cycle-analysis-of-lesmesodon-edingeri

Wilhelms-Universität Bonn, 53115 Bonn, Germany. andreas.lang@uni-bonn.de
Thomas Lehmann. Department Messel Research and Mammalogy, Senckenberg Research Institute and Natural History Museum, 60325 Frankfurt, Germany. thomas.lehmann@senckenberg.de
Thomas Martin. Section Palaeontology, Bonn Institute of Organismic Biology, Rheinische Friedrich-Wilhelms-Universität Bonn, 53115 Bonn, Germany. tmartin@uni-bonn.de

Keywords: mammal; *Lesmesodon*; Hyaenodonta; dentition; chewing cycle; Messel

Submission: 11 November 2024. Acceptance: 1 September 2025.

INTRODUCTION

Representatives of the extinct Hyaenodonta (Mammalia, Placentalia) first appeared in the fossil record at the Paleocene-Eocene transition in Asia, North America, and Europe (Borths and Stevens, 2017; Zack, 2019a) and during the late Eocene to the Oligocene, they represented one of the major groups of predatory mammals in Europe and Afro-Arabia (Borths and Stevens, 2017; Zack, 2019a). Their possible origin is still under debate with Europe, Afro-Arabia, Asia, and North America being possible (Borth and Stevens, 2017; Pfaff et al., 2017; Zack, 2019a). Hyaenodonta persisted into the late Miocene until they eventually disappeared completely with *Dissopsalis carnifex* as the last known member of this order (Barry, 1988; Egi et al., 2005).

Phylogenetic relationship of this group has been reconsidered several times and is still contentious. The original order “Creodonta” that included Hyaenodontidae is considered obsolete and Hyaenodontidae themselves are set as related but not ancestral to modern Carnivoramorpha (Halliday et al., 2017; Dubied et al., 2019; Zack, 2019b). Within Hyaenodontidae, the European Proviverrinae (e.g., *Lesmesodon* spp., *Proviverra typica*) are set either at the base (e.g., Borths and Stevens, 2019) or deeply within the hyaenodont clade (e.g., Dubied et al., 2019).

From the Paleocene until the Miocene, this group produced a variety of different forms ranging from large predators such as *Hyaenodon* to small representatives such as *Prototomus* or *Thinocyon*.

One distinct feature that is shared in hyaenodontids and carnivorans are the carnassial teeth (e.g., Solé and Ladevèze, 2017), a complex of sharp upper and lower molars and premolars used primarily for processing meat. In the Carnivoraformes this complex always consists of the upper P4 and lower m1. In juvenile crown Carnivora, the “carnassial” complex is borne by the upper dP3 and lower dp4. In comparison, hyaenodontids tend to have at the same time, multiple tooth positions with sharp crests that are considered as “carnassials”, but never the tooth pair of the upper P4 and the lower m1 (e.g., Solé and Ladevèze, 2017). In juvenile hyaenodontids, the complex in the deciduous tooth positions consists of dP3/dp4 and dP4/m1, whereas in the permanent dentitions of adults it consists of M1/m2 and M2/m3 (Figure 1) (Ungar, 2010; Bastl et al., 2011).

From an evolutionary perspective, a higher number of morphologically similar teeth offers less potential for adaptation to new ecological niches or changing environments (van Valkenburgh, 1999; Goswami et al., 2011). Modern marsupials are observed to have a similar constraint with their mode of tooth replacement, by pushing already existing teeth in anterior direction when a new molar erupts. This forces the subsequent molar to take the same shape as the previous one (Figure 1) (Werdelin, 1987). The dentition of mammals can be linked to their preferred diet, as changes in dental morphology are very often linked to shifts in dietary habits (Tamagnini et al., 2021).

Mammalian diet frequently is subject to a broad variety of studies (e.g., Merceron et al., 2007; DeSantis, 2016; Ackermans et al., 2018; Frederickson et al., 2022) and linked to the dentition in many aspects throughout species (Pineda-Muñoz et al., 2017). In recent years, 3D morphological tools, micro- and mesowear, microtexture as well as isotope analyses have become popular methods to investigate and re-evaluate dietary habits of both fossil and modern mammals (Fortelius and Solounias, 2000; Ungar, 2010; Pineda-Muñoz et al., 2017).

In this study, we pursue a dynamic 3D surface collision approach to assess the diet of the extinct proviverrine species *Lesmesodon edingeri* by simulating its chewing pattern. The stomach content of one *Lesmesodon edingeri* individual includes a small mammal and some herpetile fragment (see Gunnell et al., 2018). But this differs slightly from the suggested insect-rich diet based on tooth morphometry (Morlo and Habersetzer, 1999).

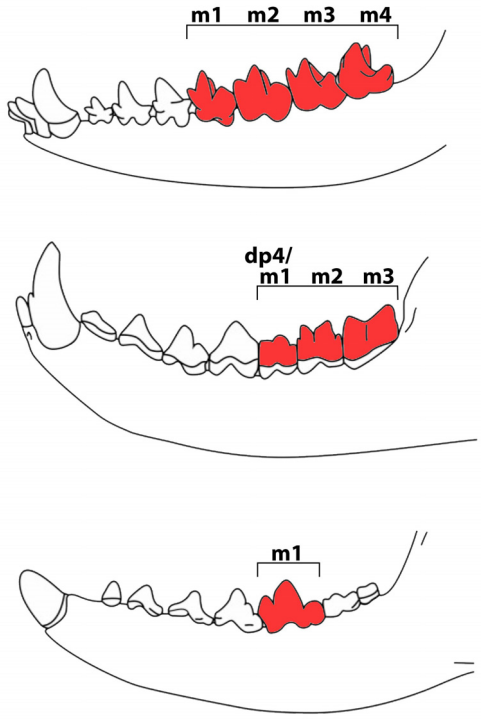

FIGURE 1. Lower toothrows in lateral view of (A) extant dasyurid marsupial *Sminthopsis*, (B) extinct hyaenodont *Hyaenodon crucians*, (C) extinct canid *Hesperocyon gregarious.* Brackets mark molar teeth, red teeth mark potential carnassials. Modified after van Valkenburgh (2007).

The goal is to establish a possible dietary range for *Lesmesodon* based on the analysis of the occurring facet patterns and a comparison to close relatives as well as modern species with known dietary habits.

Three-dimensional-modeling of tribosphenic and pretribosphenic dentitions in order to reconstruct the occlusal patterns and possible diet ranges has been done for fossil species before (e.g., Evans and Sanson, 2006; Evans and Fortelius, 2008; Jäger et al., 2019). The tool used in this study is the Occlusal Fingerprint Analyser (OFA), which has been shown to be a reliable approach to investigate chewing cycles in details (Kullmer et al., 2009).

Qualitative evaluation of facets and dynamic collision visualization with the OFA have been previously done. Schultz and Martin (2014) identified shifts in morphology and functional areas to a pure grinding phase for food comminution in the transition from the pretribosphenic molars of *Dryolestes leiriensis* to the tribosphenic molars of *Monodelphis domestica*. Likewise, Jäger et al. (2020) tested general function of the triconodont dentition of the faunivorous eutriconodontan *Priacodon fruitaensis*. By reconstructing the chewing cycle using the OFA the significant function of jaw roll and occlusal pattern of *P. fruitaensis* were revised. However, a quantitative evaluation of wear facets and duration of simulated chewing movements of fossils and extant carnivorous mammals has not been the subject of such studies yet.

With our approach, we seek to test if wear patterns seen in fossil carnivorous mammals are comparable to those seen in extant taxa with known diet. This would allow us to draw conclusions for the nutrition and food processing of the extinct taxa and to test interpretations of dietary adaptions based on tooth morphology.

MATERIAL AND METHODS

This study is based on one specimen of the hyaenodont *Lesmesodon edingeri* (HLMD-Me 14590a) from the Messel Pit fossil site (middle Eocene, Germany). The specimen is housed at the Hessisches Landesmuseum Darmstadt (HLMD). The Messel Pit offers a unique view into the Eocene epoch of continental Europe and is a place of exquisite fossil preservation due to its depositional conditions (Smith et al., 2018). The fossils from Messel are preserved in so called “oil shales”, which are bituminous pelites consisting of up to 40% water (by weight). To prevent them from drying out and disintegrating, the fossils cannot be conserved in their embedding “oil-shale” but must be transferred on an artificial resin matrix (Kühne, 1962; Ackermann et al., 1988). Since fossil vertebrates from Messel are usually found in articulation, with clenched jaws, the occlusal surface of the teeth cannot be accessed directly for study, and CT scans were used for their visualization.

High resolution epoxy casts of the molar dentitions of *Dasyurus viverrinus* (SMF_1480; Dasyuridae; Marsupialia) from the Staatliches Museum für Naturkunde Stuttgart (SNMS), of *Civettictis civetta* (ZFMK_1993_0705; Carnivora; Placentalia) from the Zoologisches Forschungsmuseum Alexander Koenig (ZFMK) and of *Sarcophilus harrisii* (ZMB_Mam_002343; Dasyuridae; Marsupialia) from the Museum für Naturkunde Berlin (MfN) were used for comparison. For this study, we also had access to an unpublished skull of *Proviverra typica* (GMH LIX-49-1992; Hyaenodontidae; Placentalia) from Geiseltal (obere Mittelkohle, middle Eocene, Germany), a close relative of *Lesmesodon* within the Proviverrinae, housed at the Zentralmagazin Naturwissenschaftlicher Sammlungen of the Martin-Luther University Halle-Wittenberg

TABLE 1. Overview of the tooth positions (TP), the collision areas (CA), and the teeth involved in the respective collision areas of each tooth position. TP 1 always corresponds to the penultimate lower molar (or dp4 in *Lesmesodon edingeri),* while TP 2 corresponds to the last lower molar position in each row of teeth for each species.

Tooth Position (TP)	Teeth involved in Collision Area (CA)		
L. edingeri	CA1	CA2	CA3
TP1	dp4/dP3	dp4/dP4	dp4/dP4
TP2	m1/dP4	m1/M1	m1/M1
P. typica			
TP1	m2/M1	m2/M2	m2/M2
TP2	m3/M2	m3/M3	m3/M3
D. viverrinus			
TP1	m3/M2	m3/M3	m3/M3
TP2	m4/M3	m4/M4	m4/M4
C. civetta			
TP1	m1/P4	m1/M1	m1/M1
TP2	m2/M1	m2/M2	m2/M2
S. harrisii			
TP1	m3/M2	m3/M3	m3/M3
TP2	m4/M3	m4/M4	m4/M4

(GMH). To make the analysis of the chewing cycles comparable, only parts of toothrows of adult specimens with complete molar dentition (m1-3, M1-3) were chosen (see Table 1), except for *L. edingeri* which bears a subadult dentition. The dentition of this subadult specimen was chosen, because between the three µCT-scanned specimens of *Lesmesodon* available, this was the only specimen with preserved protocones in the upper molars.

For this study a “complex” refers to the functional unit of the two tooth positions (**TP**).

TP indicates which lower molar is currently meant, while “complex” means the functional unit with either one or both upper molars involved (Table 1). Collision Area (**CA**) refers to the collision surface that could be traced on the facets of the involved teeth (Table 1). For tooth nomenclature we follow Rich (1981) (Figure 2).

All specimens were µCT-scanned and 3D models were reconstructed for the analysis. Specimens HLMD-Me 14590a and GMH LIX-49-1992 were scanned using a Tomoscope HV500 (Werth Messtechnik GmbH) at the Fraunhofer Application Center for CT in Metrology (CTMT) at the Deggendorf Institute of Technology (Table 2). The specimens of *D. viverrinus, C. civetta* and *S. harrisii* were scanned with the v|tome|xs µCT device (GE Sensing & Inspection Technologies GmbH phoenix|x-ray) housed at the Bonn Institute for Organismic Biology, Section Paleontology, University of Bonn, Germany (Table 2).

For segmentation, Avizo Lite 2020.2. (build 2020-06-03) was used. The default rendering settings were chosen, and the smoothing level was set to 3, in order not to lose too much surface information. The rendered models were exported as STL (Little Endian) files. The exported models were edited (e.g., holes closed, cracks patched, broken cusps reconstructed) using the IMEdit module of Polyworks 2014 IR13 (build 5872) software package. Editing was held to a minimum, to be as close to the original surface as possible. Edited models were then imported into the Occlusal Fingerprint Analyser (OFA) (version 2, build 1810 x86_64). The OFA is a freely downloadable software (https://www.paleontology.uni-bonn.de/de/forschung/ehemalige-forschergruppen/for-771-ofa/occlusal-fingerprint-analyser-ofa) developed by the DFG (Deutsche Forschungsgemeinschaft) research unit 771 (Kullmer et al., 2009; Martin and Koenigswald, 2020). The software is primarily used for reconstructing jaw movements during the power stroke of the chewing cycle detecting collisional contacts during occlusion. Within the program, chewing motions can be reconstructed, surface collisions detected as well as visualized and analyzed. By following a user-introduced trajectory, a computer-based simulation of the chewing path is calculated as well as the position and orientation of antagonistic wear facets simulated by collision of the 3D surfaces. Reconstruction of the collision paths for extant species is done with the help of

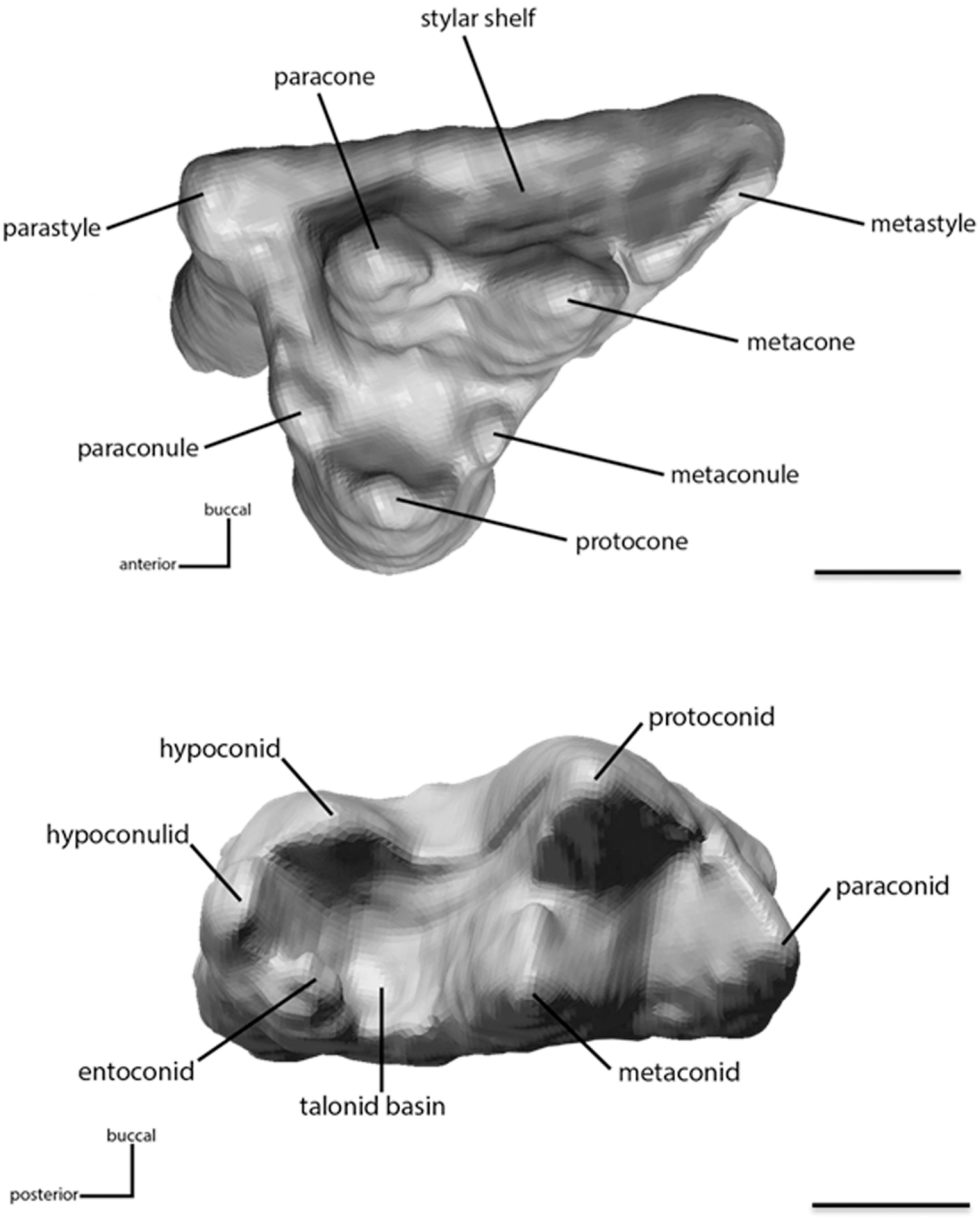

FIGURE 2. Occlusal view of sinistral upper dP4 and lower m1 of *Lesmesodon edingeri* (sinistral) with the most important structures marked. Nomenclature follows Rich (1981). Scale bar equals 1 mm.

high detail casts that preserve attrition and abrasion facets. These are used as a basis for relative movements that aid to create the general directions of the user introduced trajectory. The detailed pathway is then calculated using the 'octree kdtree threaded pool list global' algorithm of the software. The standard settings for collision distance were set as 0.25 and trajectory approximation was e^x= 5. Deflection angle was set smaller than 72° and given degree steps for break free were set to 10. Maximum degree for break free was set to 350. For contact detection a distance of 0.2 mm is chosen and the distance between each calculated point along the collision path is set to 0.01 mm.

For comparison between taxa, indices are calculated to present the results as independently as possible. For the collision size index, the maximum collision area of the individual areas (CA 1-3) is compared with the largest total collision that occurs on the respective teeth during the chewing cycle. The collision duration index is calculated by comparing the duration-in steps-of the individual collision area and the total number of calculated steps with existing collisions on the toothrow. Further, for

TABLE 2. Parameters for µCT-scans of each specimen.

***Lesmesodon edingeri* (HLMD-Me 14590a)**	
Voxelsize:	45.3µm
Voltage:	150kV
Current:	250µA
Steps	1600
***Proviverra typica* (GMH LIX-49-1992)**	
Voxelsize:	20.1µm
Voltage:	220kV
Current:	100µA
Steps:	1600
***Dasyurus viverrinus* (SMF_1480)**	
Voxelsize:	40.1µm
Voltage:	110kV
Current:	110µA
Timing:	400ms
***Civettictis civetta* (ZFMK_1993_0705)**	
Voxelsize:	78.4µm
Voltage:	110kV
Current:	110µA
Timing:	500ms
***Sarcophilus harrisii* (ZMB_Mam_002343)**	
Voxelsize:	44.1µm
Voltage:	120kV
Current:	350µA
Timing:	333ms

each specimen an active and complete Cutting-Edge-Index (CEI, cutting edge length/tooth length) is formed. For the CEI, the metacrista (=post-metacrista) and paracristid which are involved in the shear-cutting function are measured. The "complete CEI" includes the whole length of these measured edges, the "active CEI" describes the part of the edge that shows collisions as simulated by the OFA (Figure 3).

RESULTS

The OFA reconstructed chewing path for each specimen has been modelled as a trajectory with the upper molar series remaining static while the lower molar series is moving towards them in apical direction, as it is in the actual mammalian chewing pattern. The trajectories visualized using the OFA are based on the movement with teeth in full occlusion and therefore reflect the actual power stroke.

Collision Detection

Following Hiiemae and Kay (1972) the chewing cycle can generally be separated into two phases of the power stroke (teeth in occlusion). Phase I represents the closing of the jaw until maximum intercuspation of the teeth is reached (Hiiemae and Kay, 1973). During this phase, the mechanical processes of shearing, cutting, and crushing are the primary active functions. While in phase II the jaw opens again, and grinding is taking over as the main function in action (Shimizu et al., 2005). The "highest" point in the OFA reconstructed masticatory path marks the point of maximum intercuspation and the end of phase I in the chewing cycle. At the same time, it also marks the beginning of phase II of the chewing cycle. The trajectories visualized using the OFA are based on the movement with teeth in full occlusion and therefore reflect the actual power stroke.

Contact duration and relative collision area differ between taxa as detected by the OFA. The analysis shows how the chewing cycles in insectivorous species (e.g., *Lesmesodon edingeri, Proviverra typica,* and *Dasyurus viverrinus*) appear to be shorter than in the hypercarnivorous *Sarcophilus harrisii* or the omnivorous *Civettictis civetta* (Figure 4, see *1). In addition, contact areas of insectivorous species investigated here seem to build up faster and in a shorter time (Figure 4). First contact and therefore first rise in slope of the graphs (Figure 4, see *1) is almost exclusively between the metacrista and paracristid. Protocrista and protocristid follow as colliding structures, increasing the slope rise even further. In *Lesmesodon edingeri*, the initial growth in contact area is, unlike in the others, formed by the protocrista and protocristid while metacrista and paracristid are responsible for the second increase (due to additional collision area of the protocone occluding into the talonid basin; Figure 4, see *2), together with the protocone, which begins to occlude into the talonid basin. The occluding protocone inside the talonid is also the main cause for the second rise of collision area in *P. typica, D. viverrinus* and *C. civetta* (Figure 4, see *2), while the occlusion of the paracone into the hypoflexid could be identified as an additional cause. In the insectivorous taxa, the highest amount of surface collision happens at the point of maximum intercuspation, when occlusion of the protocone into the talonid basin is deepest in combination with the blades of metacrista/paracristid in collision. In comparison, the largest collision area for *S. harrisii* appears early, during phase I of the chewing cycle (Figure 4, see *3), represented

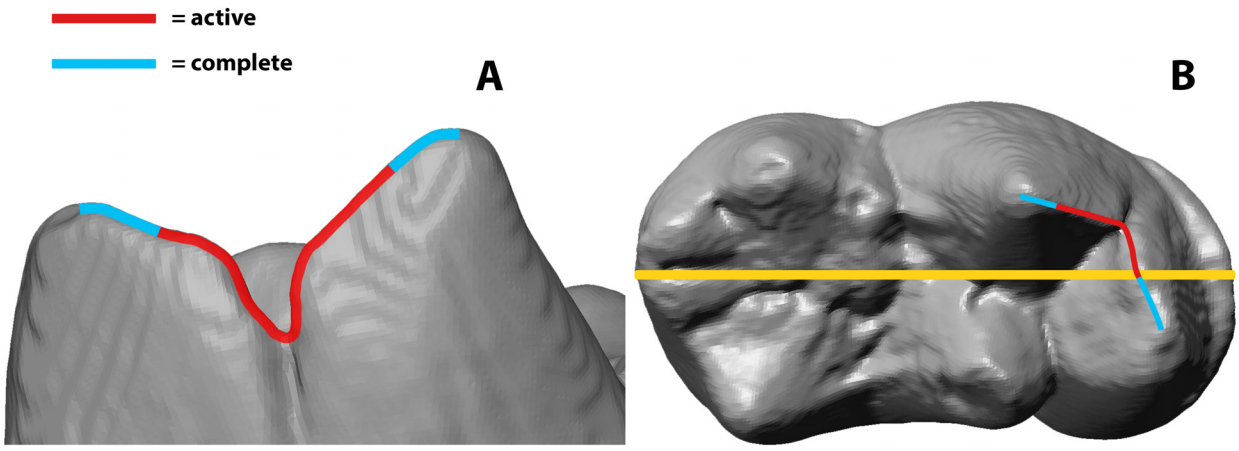

FIGURE 3. Exemplary representation of how the Cutting-Edge-Index (CEI) is calculated. Measurements are taken in PolyWorks during the chewing cycle, for the active (red line) and the complete (blue lines) edge of the paracristid. This length is then divided by the complete length of the respective tooth (yellow line). (A) anterobuccal view of the m1 of the paracone and protocone of *Civettictis civetta*, (B) Occlusal view of the m1 of *C. civetta*. Not to scale.

by the maximum peak of the curve involving only metacrista and paracristid. In *C. civetta* the largest collision area appears during the transition of the paracrista/protocristid collision to the occlusion of the protocone into the talonid basin (Figure 4, see *4). In Phase II all surface collisions decrease shortly after the maximum intercuspation in all species except for *S. harrisii*, where the surface collision is at its lowest at the point of maximum intercuspation. The drop is caused primarily by detachment of the facets along metacrista/paracristid moving out of occlusion and the protocone moving through the talonid basin in posterior-buccal direction, moving away from the posterior side of the meta- and protoconid. In the insectivorous "species" the protocone moves completely through the talonid basin, eventually colliding with the entoconid and hypoconulid before moving out of the basin.

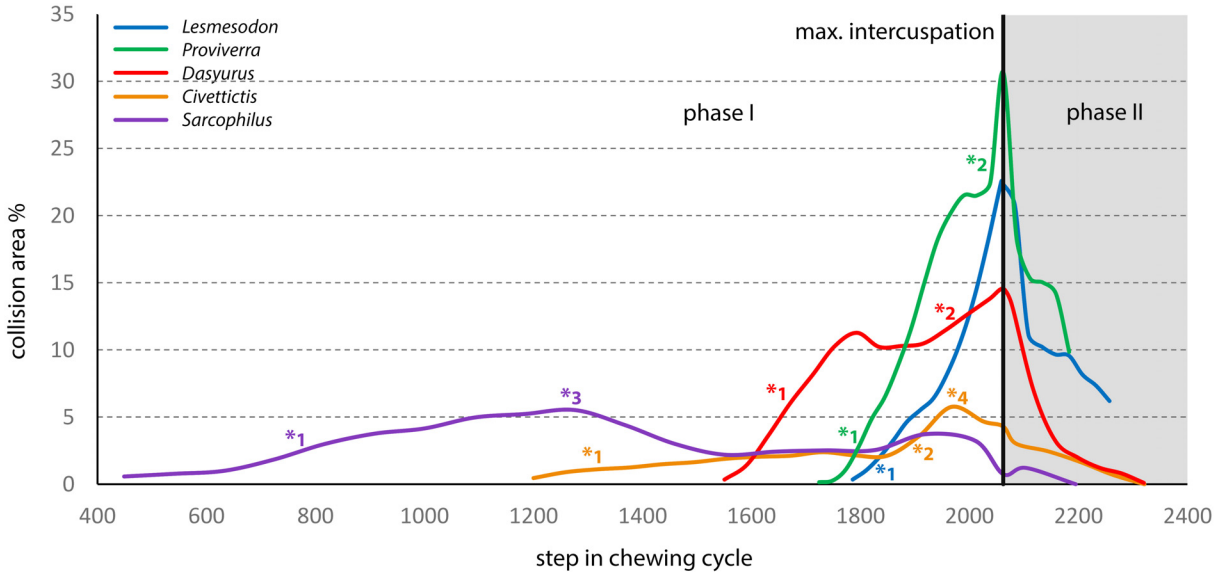

FIGURE 4. Chewing cycles of all compared species, calibrated to the point of maximum intercuspation. *Lesmesodon edingeri* and *Proviverra typica* show similar graphs and, including *Dasyurus viverrinus*, have their point maximum surface collision in the position of central occlusion. In every species phase I is noticeably longer than phase II.

Masticatory System Movement

Lesmesodon edingeri. The calculated path for phase I starts in 90° vertical direction following a trajectory slightly inclined by ~15° in mesial direction. The movement along the path increases in inclination of ~2° to the lingual side in addition to a mesial tilting halfway up to the point of maximum intercuspation. Before maximum intercuspation is reached, the angle of the collision path inclined is deflected and further inclines in mesial direction to ~75°. A transverse component is added to the movement, with a lingual inclination of ~25° until the highest point (maximum intercuspation) is reached. From this point the chewing cycle enters phase II. For a short duration, the masticatory path is horizontal and moves in postero-buccal direction. The path then tilts downward with ~55° until no further collisions are detected (for visualization of the movement see Appendix 1).

Proviverra typica. Occlusion starts with initial trajectory of the path tilting in an angle of ~45° in lingual of ~35° in anterior direction. There was no directional change detected during the entire phase I of the chewing cycle. After the point of maximum intercuspation, in phase II, the calculated path starts oriented in ventral direction by ~30°, while the angle of the anterior movement increases to a total of now ~50°. Finally, the angle in anterior direction raises to an angle of ~65° until all detected collisions end (for visualization of the movement see Appendix 2).

Dasyurus viverrinus. The initial occlusal contact in the chewing path occurs during a calculated tilt in lingual direction at an angle of ~35° with a slight posterior component of ~5°.

At the highest point, the calculated path tilts briefly ~20° in ventral direction. After a short duration, maximum intercuspation is reached and the masticatory path flattens to an almost horizontal movement. The masticatory path enters phase II. From here the path changes to a ventral direction of 60°, until all detected collisions end (for visualization of the movement see Appendix 3).

Sarcophilus harrisii. The calculated path starts from an angle of ~28° in lingual direction. After one quarter of the chewing path, the angle changes to ~5° in ventral direction with slightly posterior orientation. Right before the last quarter, the calculated path changes its direction and moves in a slightly s-shaped way in anterior direction. Phase I of the calculated path ends with tilting slightly into ventral direction with ~5°, then changing back to ~18° in apical direction for a short stretch until maximum intercuspation is reached. The masticatory path flattens during phase II but continues in an angle of ~15° viewed from horizontal plane in lingual direction until the collisions end (for visualization of the movement see Appendix 4).

Civettictis civetta. The calculated path starts in anterior direction with > 10° and with ~30° in lingual direction. Halfway to maximum intercuspation, the calculated path changes slightly into an anterior-lingual direction. Reaching maximum intercuspation, the angle of the calculated path flattens by ~40° but keeps its anterior-lingual direction. In the beginning of phase II, the collision path changes direction slightly ventral and flattens to ~5°. The calculated path tilts further ventral by 15°. It keeps this ventral tilt and its anterior-lingual direction until no further collisions are detected (for visualization of the movement see Appendix 5).

Collision Area Comparison

The before-mentioned structures (metacrista, protocrista, paracrista, paracristid, protocristid, protocone, and talonid basin) are primarily responsible for the peaks in the chewing cycle, form the largest collision areas (CA) on the tooth surfaces and are therefore involved in a large part of the food processing. Taking a closer look at these areas in terms of size and their collision duration during one chewing cycle could provide detailed insights on further food processing of each taxon. In each taxon, the occurring collision areas can be separated into three main areas per tooth.

Collision Area 1 (CA 1) exists between the metacone, metacrista, and metastyle and the paraconid, paracrista, and protoconid (Figures 5 - 9). It is rather small in the extinct species (Figure 4a). *Lesmesodon edingeri* builds a smaller CA than *Proviverra typica* (Figures 10A, 11A), and the duration of this CA during one chewing cycle is almost twice as long in the latter, showing some of the longest durations observed (Figure 11B). *Dasyurus viverrinus* shows a CA size larger than *L. edingeri* but not as long lasting in collision duration as in *P. typica* and lies in between the other insectivorous species (Figures 10, 11). In *C. civetta* we see long CA duration (Figure 10B) but small CA size. *Sarcophilus harrisii* shows long duration and size in this CA (Figures 10, 11).

Collision Area 2 (CA 2) exists between the mesial side of the protocone and the protoconid, protocristid, and metaconid (Figures 5-9). It shows highest values for both collision duration and size for *L. edingeri* and is in fact the longest in *L. edingeri* compared to all other taxa (Figures 10, 11).

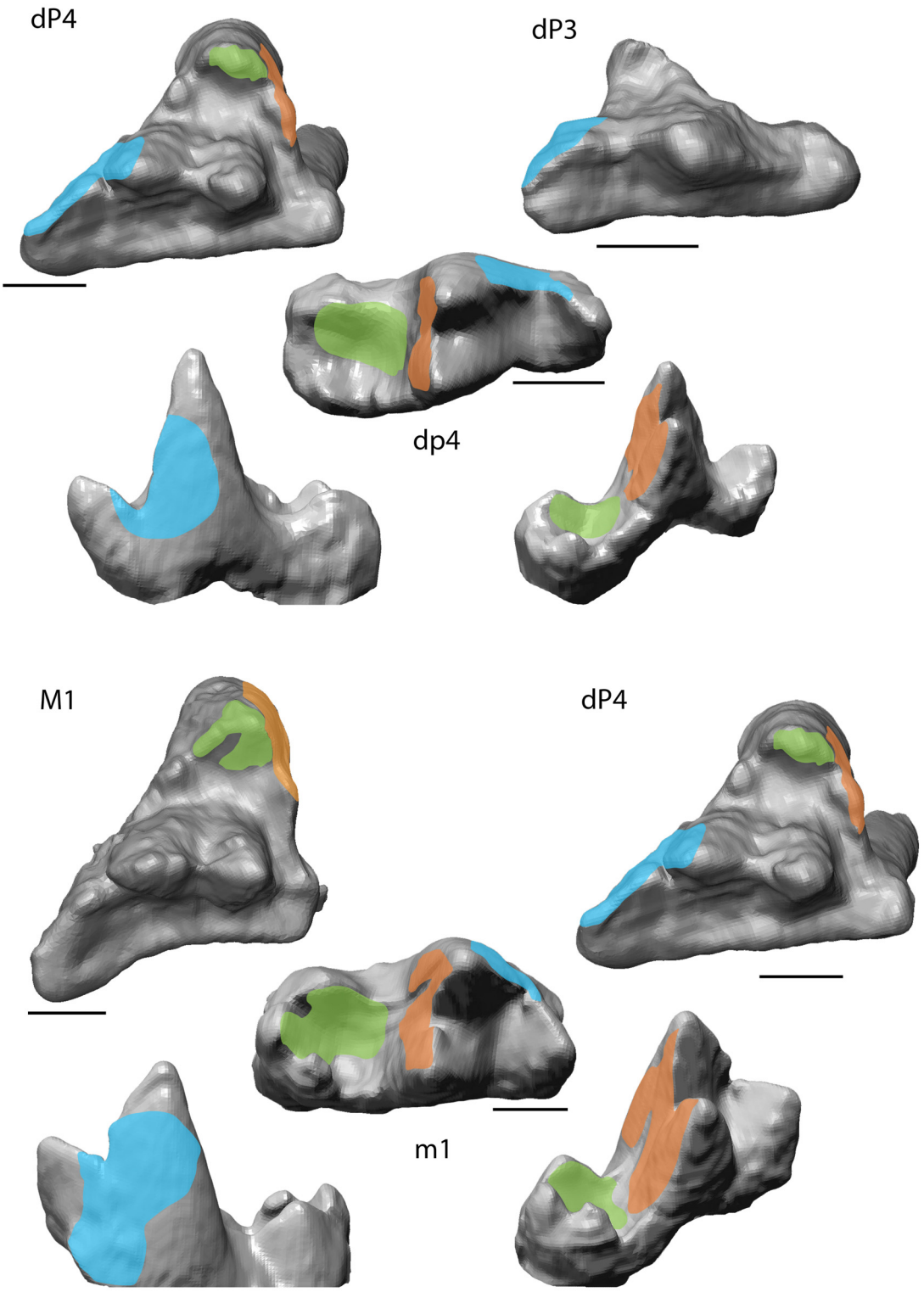

FIGURE 5. Collision areas (CA) of *Lesmesodon edingeri* (HLMD-Me 14590a) detected by the OFA - analysis for the three discussed main CAs 1-3 for the TP 1, TP2 complex. Lower molar is shown (from left to right) in anterobuccal view, occlusal view and posterolingual view. CA 1 shown in blue, CA 2 shown in orange and CA 3 shown in green. Scale bar equals 1 mm.

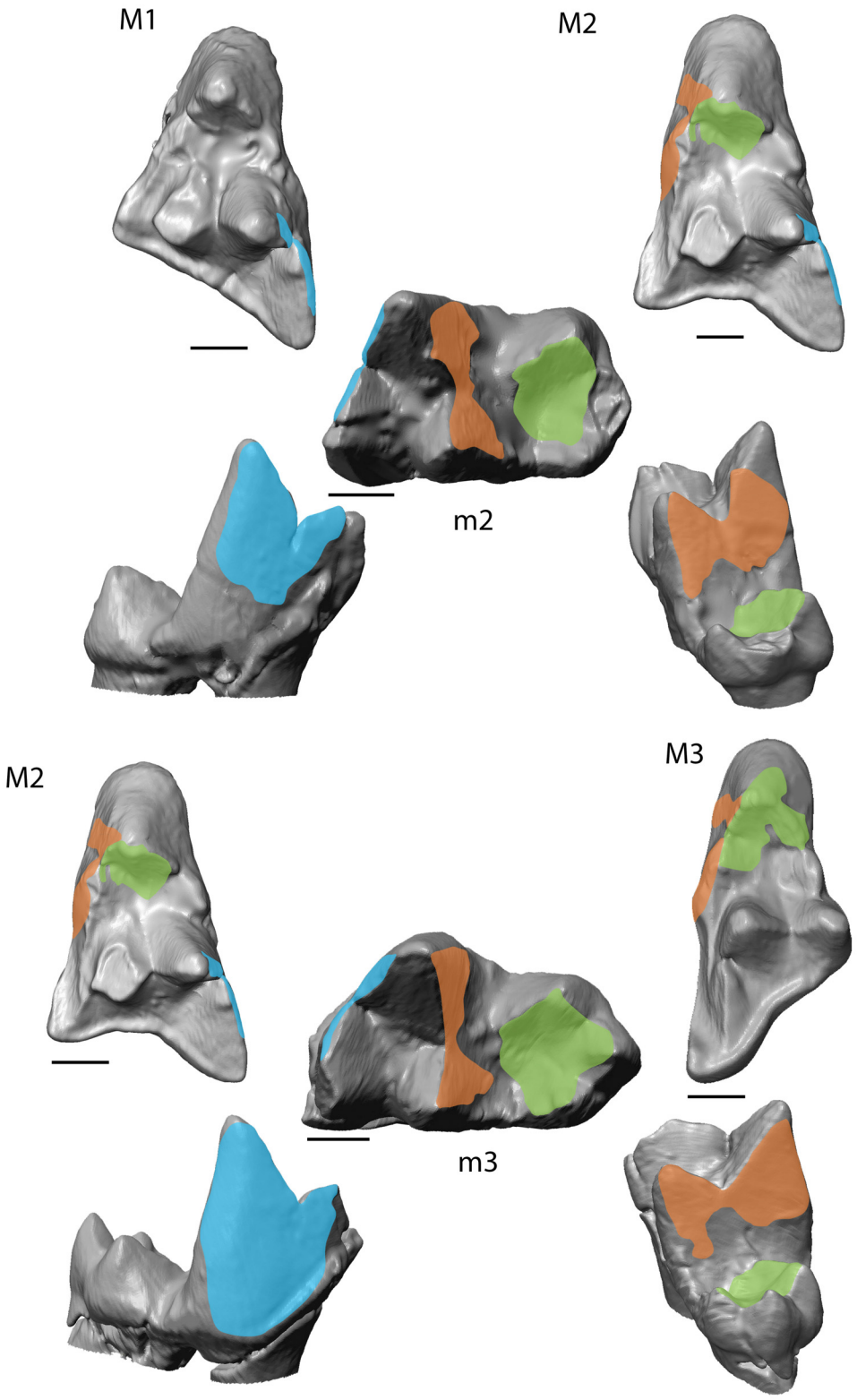

FIGURE 6. Collision areas (CA) of *Proviverra typica* (GMH LIX-49-1992) detected by the OFA - analysis for the three discussed main CAs 1-3 for the TP 1, TP2 complex. Lower molar is shown (from left to right) in anterobuccal view, occlusal view and posterolingual view. CA 1 shown in blue, CA 2 shown in orange and CA 3 shown in green. Scale bar equals 1 mm.

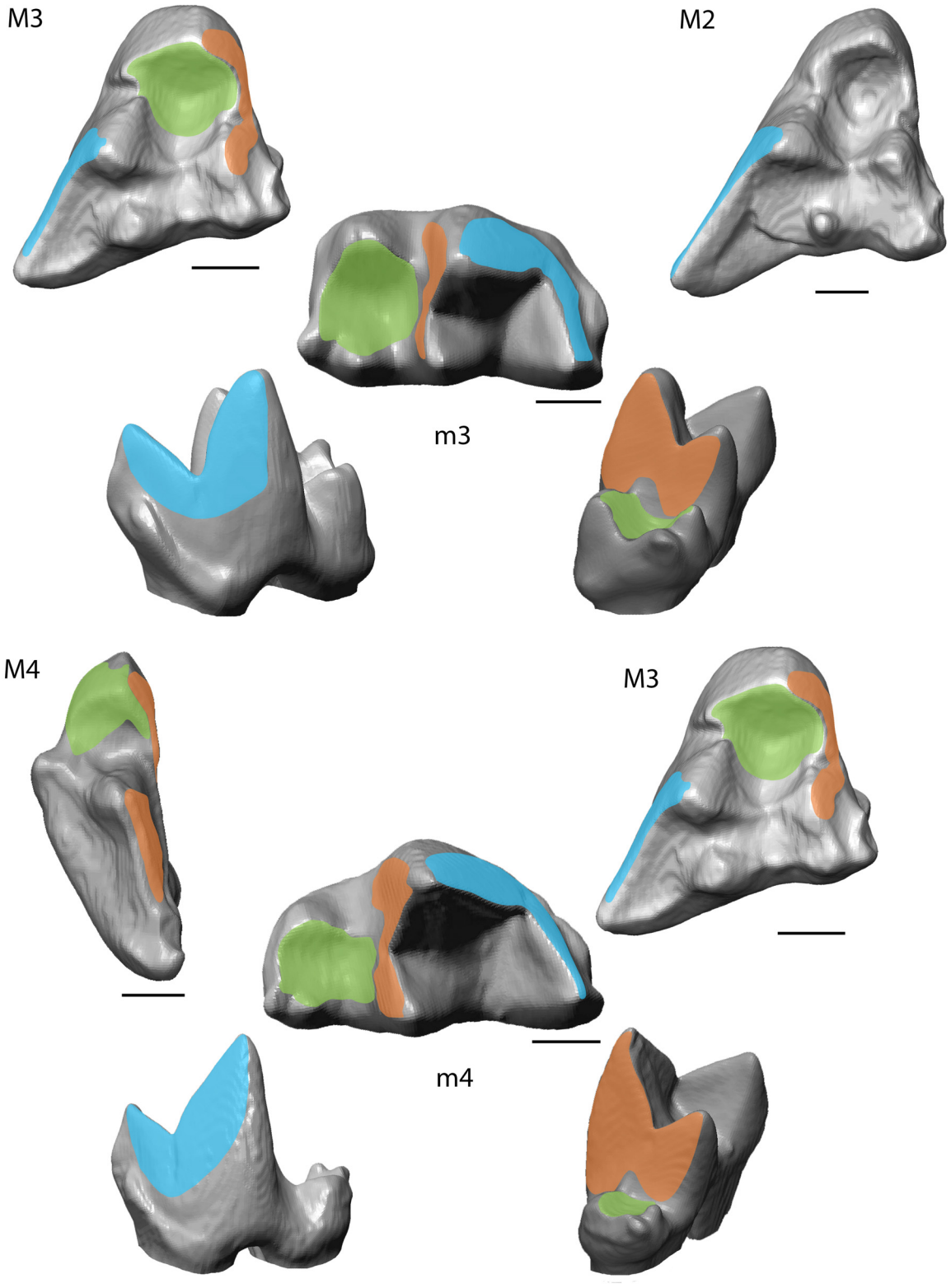

FIGURE 7. Collision areas (CA) of *Dasyurus viverrinus* (SMF_1480) detected by the OFA-analysis for the three discussed main CAs 1-3 for the TP 1, TP2 complex. Lower molar is shown (from left to right) in anterobuccal view, occlusal view and posterolingual view. CA 1 shown in blue, CA 2 shown in orange and CA 3 shown in green. Scale bar equals 1 mm.

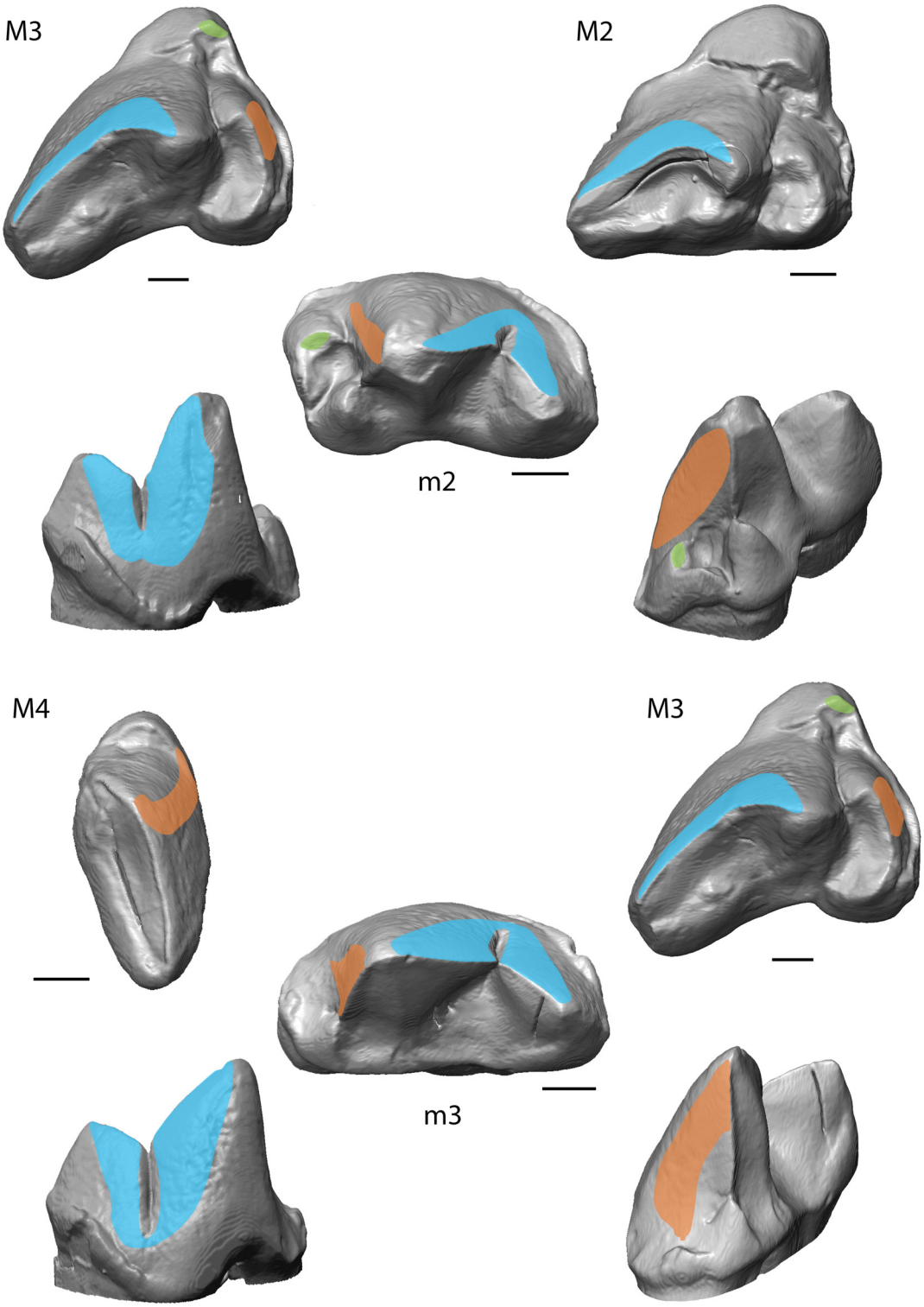

FIGURE 8. Collision areas (CA) of *Sarcophilus harrisii* (ZMB_Mam_002343) detected by the OFA - analysis for the three discussed main CAs 1-3 for the TP 1, TP2 complex. Lower molar is shown (from left to right) in anterobuccal view, occlusal view and posterolingual view. CA 1 shown in blue, CA 2 shown in orange and CA 3 shown in green. Scale bar equals 2 mm.

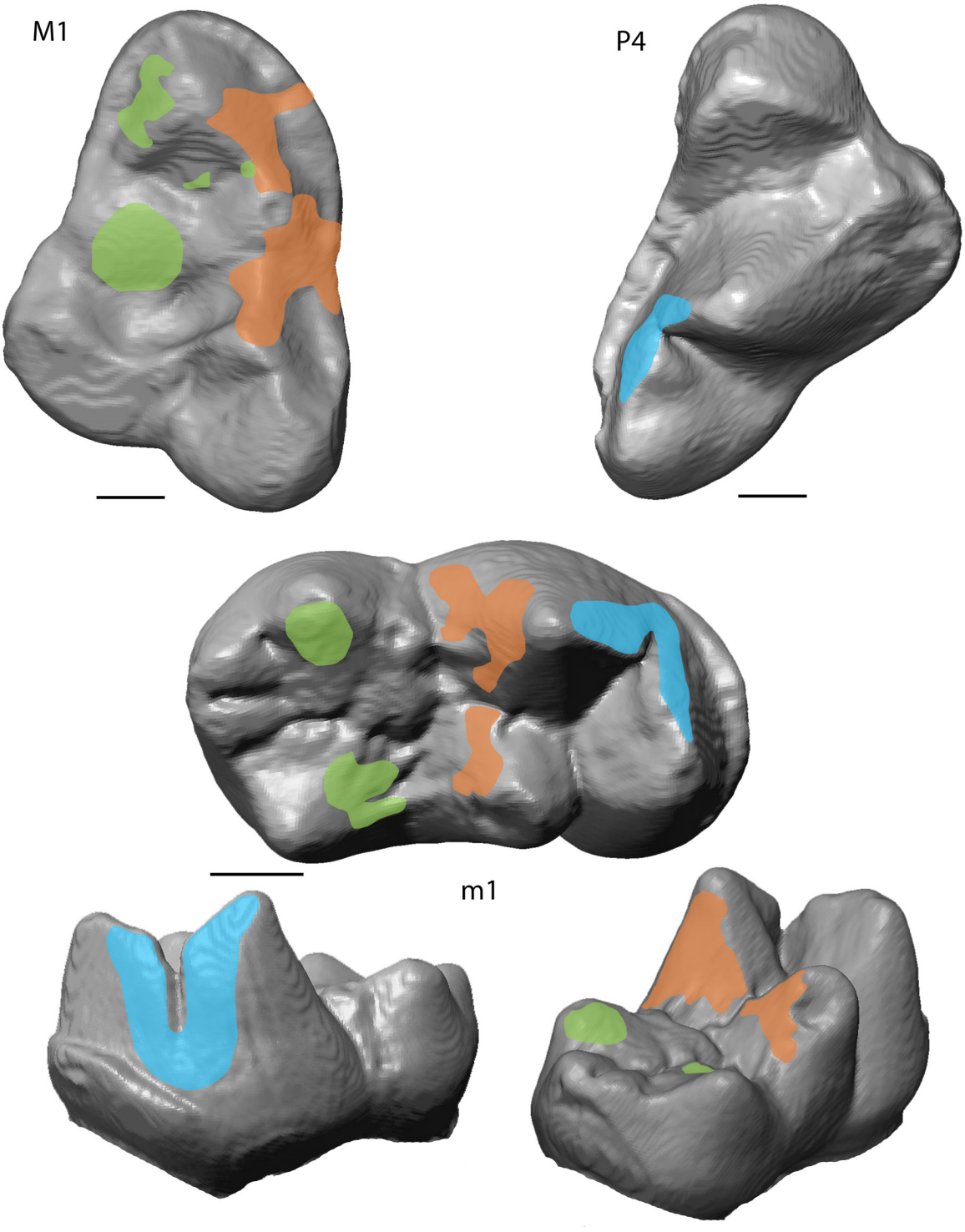

FIGURE 9. Collision areas (CA) of *Civettictis civetta* (ZFMK_1993_0705) detected by the OFA - analysis for the three discussed main CAs 1-3 for the TP 1, TP2 complex. Lower molar is shown (from left to right) in anterobuccal view, occlusal view and posterolingual view. CA 1 shown in blue, CA 2 shown in orange and CA 3 shown in green. Scale bar equals 2 mm.

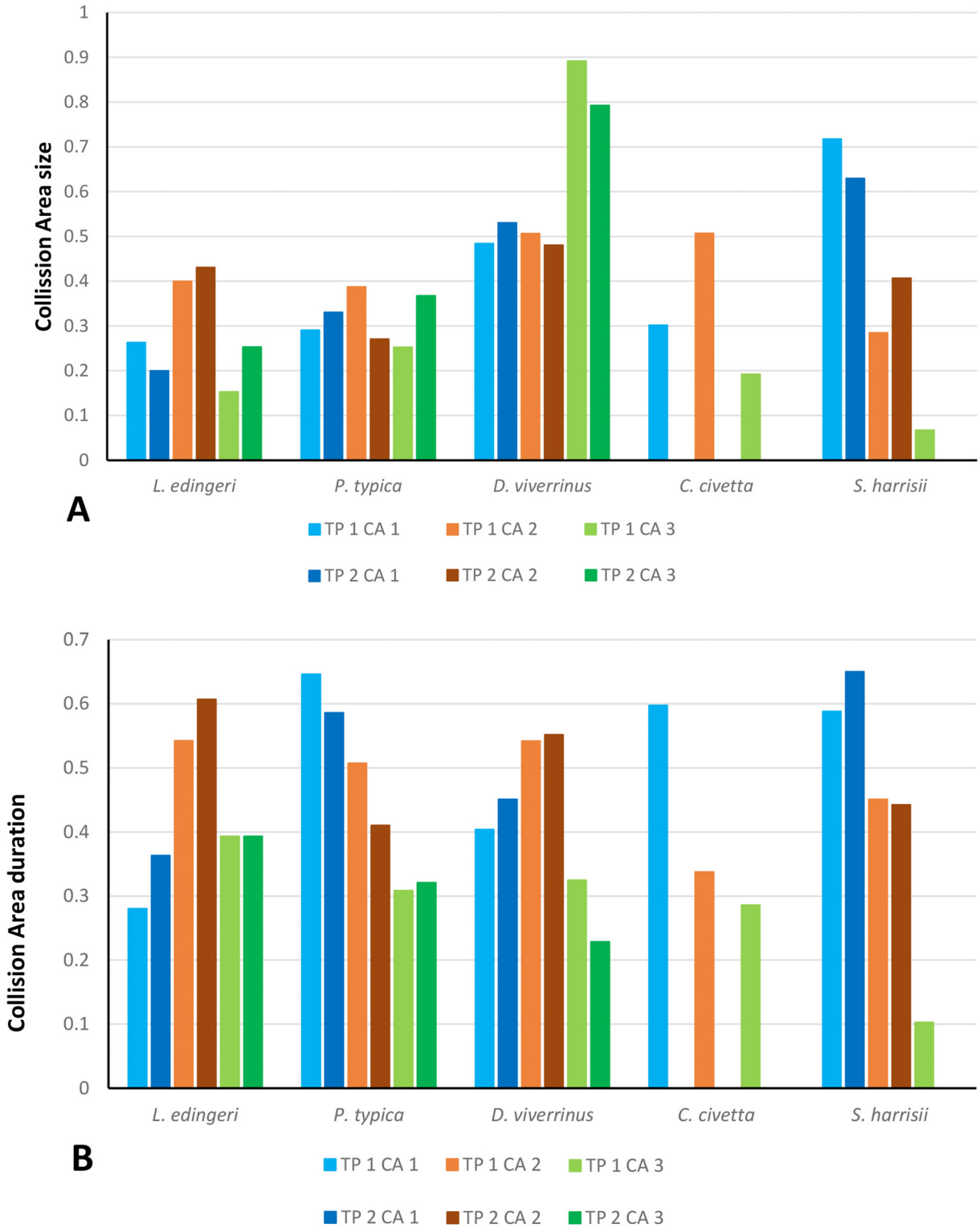

FIGURE 10. Single values for (A) Collision Area (CA) size and (B) Collision Area duration for each individual molar over the course of one single chewing cycle. The maximum CA size is in relation to the overall collision. TP 1 marks the first lower molar of each complex, TP 2 marks the second lower molar.

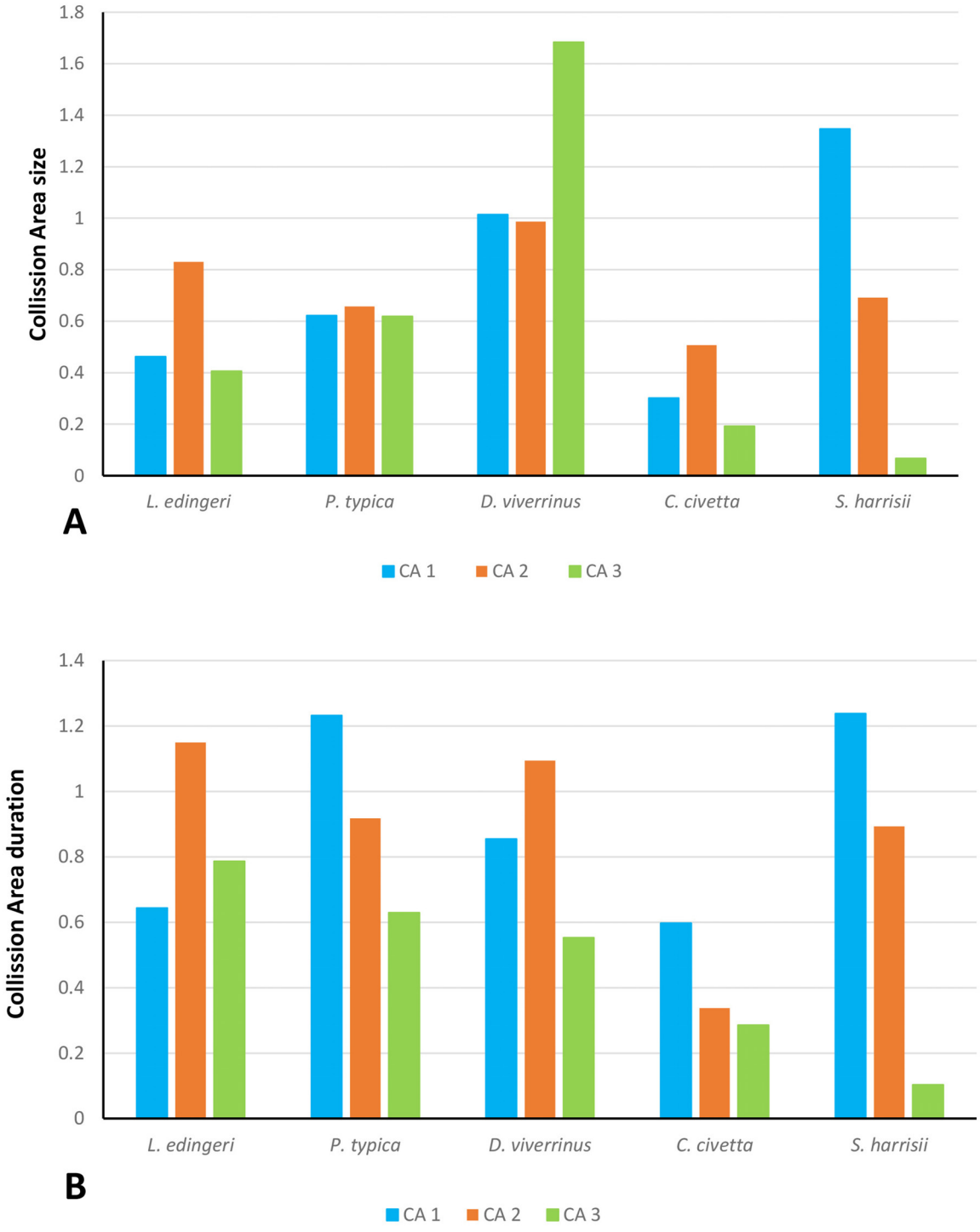

FIGURE 11. Combined percentage values for (A) Collision Area (CA) size and (B) CA duration over the course of one chewing cycle.

The size of CA 2 in *P. typica* is small but long lasting. In *D. viverrinus* CA 2 is almost identical in size to CA 1. Durations are a bit higher in CA2 but even between different tooth positions (TP, see Table 1) the values differ only little (Figures 10, 11). *Civettictis civetta* shows one of the largest CA 2 on the TP 1 but at the same time one of the shortest durations (Figures 10A, B). *Sarcophilus harrisii* lies somewhat in the middle of all taxa concerning size and collision duration (Figures 10, 11).

Collision area 3 (CA 3) exists between the protocone and the talonid basin (Figures 5-9). It often seems to be the smallest CA in both duration and size. Especially in *S. harrisii* the CA 3 seems to have almost no impact on food reduction over one chewing cycle (Figures 10, 11). In *L. edingeri* the collision duration of CA 3 is longer lasting than CA 1 and in *D. viverrinus* CA 3 is larger than CA 1 or CA 2. (Figures 10A, 11A).

Cutting-Edge-Index (CEI)

Lesmesodon edingeri shows some of the smallest CEIs in both upper/lower molars or active/complete CEI (Tables 3, 4). Even though the lower molar complete CEIs are similar to those of *Proviverra typica*, the active CEIs of *L. edingeri* generally show lower values (Tables 3, 4). *Proviverra typica* and *Dasyurus viverrinus* differ in their active and complete CEIs between lower and upper jaw. *Proviverra typica* shows the highest active and complete CEI in the upper molars, this is in contrast with the lower molars (Tables 3, 4). *Dasyurus viverrinus* has, apart from the active CEIs of the upper molars, high active and complete CEIs often comparable to *Sarcophilus harrisii. Dasyurus viverrinus* however shows low variability among the CEIs of the single teeth, while in *S. harrisii* the complete CEI can differ significantly between single TPs (Tables 3, 4). Active CEI in *L. edingeri* tends to vary more than in the other species and has a high deviation. A certain degree of varaition can also be found in *S. harrisii* and *P. typica*. While deviation in the upper molars is similar in all TPs in *P. typica*, the difference between active and complete CEI in the lower molars is high in *S. harrisii* while remaining low in its upper molars (Tables 3, 4). In *Civettictis civetta* the active CEI is always much lower than the complete CEI. In general, active and complete CEIs in the lower molars of *C. civetta* remain low. In sum, *L. edingeri* is positioned at the low end of the range of variability in CEIs, whereas *S. harrisii* tends to show the highest variability in both CEIs regardless of active/complete CEI or upper/lower molars. *Dasyurus viverrinus* and *P. typica* change their position between upper and lower jaw, whereas *C. civetta* always has a much higher complete than active CEI (Tables 3, 4).

DISCUSSION

Dynamic wear facet studies provide new insights into the function of teeth, because they are directly related to the processing of food items. Facets (in their static appearance) are light reflecting, polished surface areas on the teeth resulting from attrition or abrasion during the breakdown of

TABLE 3. CEI for the upper molars. The active CEI is the part of the carnassials that is actively used during the power stroke, while the complete CEI is describes the complete length of the edges. *Proviverra typica* shows an especially high index, with *Sarcophilus harrisii* on the expected upper end as well.

	Upper Molars				
	L. edingeri	***P. typica***	***D. viverrinus***	***C. civetta***	***S. harrisii***
dP3 active	0.266	0	0	0	0
dP4 active	0.630	0	0	0	0
P4 active	0	0	0	0.545	0
M1 active	0	1.008	0	0	0
M2 active	0	0.817	0.493	0	0.676
M3 active	0	0	0.492	0	0.721
dP3 compl.	0.527	0	0	0	0
dP4 compl.	0.630	0	0	0	0
P4 compl.	0	0	0	0.744	0
M1 compl.	0	1.199	0	0	0
M2 compl.	0	1.054	0.638	0	0.698
M3 compl.	0	0	0.667	0	0.721

TABLE 4. CEI for the lower molars. The active CEI is the part of the carnassials that is actively used during the power stroke, while the complete CEI is describes the complete length of the edges. *Sarcophilus harrisii* shows the highest value while *Lesmesodon edingeri* and *Civettictis civetta* are positioned at the lower end.

	Lower Molars				
	L. edingeri	***P. typica***	***D. viverrinus***	***C. civetta***	***S. harrisii***
dP4 active	0.496	0	0	0	0
m1 active	0.304	0	0	0.345	0
m2 active	0	0.563	0	0	0
m3 active	0	0.567	0.669	0	0.729
m4 active	0	0	0.721	0	0.685
dP4 compl.	0.582	0	0	0	0
m1 compl.	0.531	0	0	0.552	0
m2 compl.	0	0.563	0	0	0
m3 compl.	0	0.567	0.798	0	1.060
m4 compl.	0	0	0.817	0	0.742

food items (Koenigswald, 2018). Data on facet size in a dynamic chewing context are rare and their duration within an active mastication process in living species might reveal dietary adaptations, that can be used to make inferences for fossil taxa. For example, *Dasyurus viverrinus* is primarily insectivorous while *Civettictis civetta* represents a taxon with an omnivorous diet, and *Sarcophilus harrisii* has a hypercarnivorous/durophagous diet. Their diets are well documented. Comparing their chewing and dynamic facet patterns with those of extinct species allows for the identification of functional similarities and differences from fossil species. Here, we describe the chewing patterns and facet collisions detected during occlusion of existing species with a known diet and compare them to that of extinct taxa to test the assumption, that the OFA can serve as a tool for dietary assumptions and aim to draw conclusions about their dietary adaptions.

Collision Areas

The analyzed upper tooth row consists of dP3, dP4, M1, and dp4, m1 in HLMD-Me 14590a. CA 1 is the second smallest in *Lesmesodon edingeri*. Other specimens of *L. edingeri* species have been shown with the M2 in the process of eruption (Morlo and Habersetzer, 1999; Bastl and Nagel, 2014; Solé et al., 2021), which implies that the individual studied here was in a relatively juvenile stage with deciduous teeth still functional. The values for CA 2 are higher, indicating that this collision area is more functional in both collision duration and contact area than CA 1 (Figures 10, 11). The values for CA 2 are comparable to those of insectivorous species (*Proviverra typica* and *Dasyurus viverrinus*) with primarily shear-cutting function and has only a slightly shorter duration (Figures 12, 13). This suggests that in juvenile *L. edingeri* the primary carnassial function, at least in the deciduous dentition, was not between metastyle/metacrista and paracristid, as in the other taxa of this study, but between the protocrista and the protocristid. In the TP 1 complex, the paraconid of dp4 is lower compared to the metaconid and the protoconid of the m1 of the TP 2 complex. However, in both TPs the paracristid-important for CA 1-fulfills a carnassial-like function somewhat later within the chewing cycle. Shares in size and duration between the CAs remain more or less equal between TP 1 and TP 2, while the involvement of the lower permanent molar seems to have little effect on CA shares. The values for shear-cutting between two permanent carnassial teeth in *L. edingeri* and its effect on values in CA 1 remain unknown, since they have not erupted in the individual that was available for the study.

The dentition of *Proviverra typica* shows a different result. CA 1 of the carnassials shows stronger involvement in collision duration than seen in *L. edingeri* (Figures 10, 11). Its size though does not exceed that of CA 2 like in a more carnivorous dentition (e.g., *Sarcophilus harrisii*) (Figure 11). However, primary shear-cutting function seems to lie within CA 1 rather than CA 2 as its duration is somewhat longer. *Dasyurus viverrinus* is the only taxon in which CA 3 surpasses the duration of the other CAs. In combination with almost equal sizes of CA 1 and CA 2, it suggests an emphasis for food processing inside the talonid basin compared to the other taxa (Figure 11).

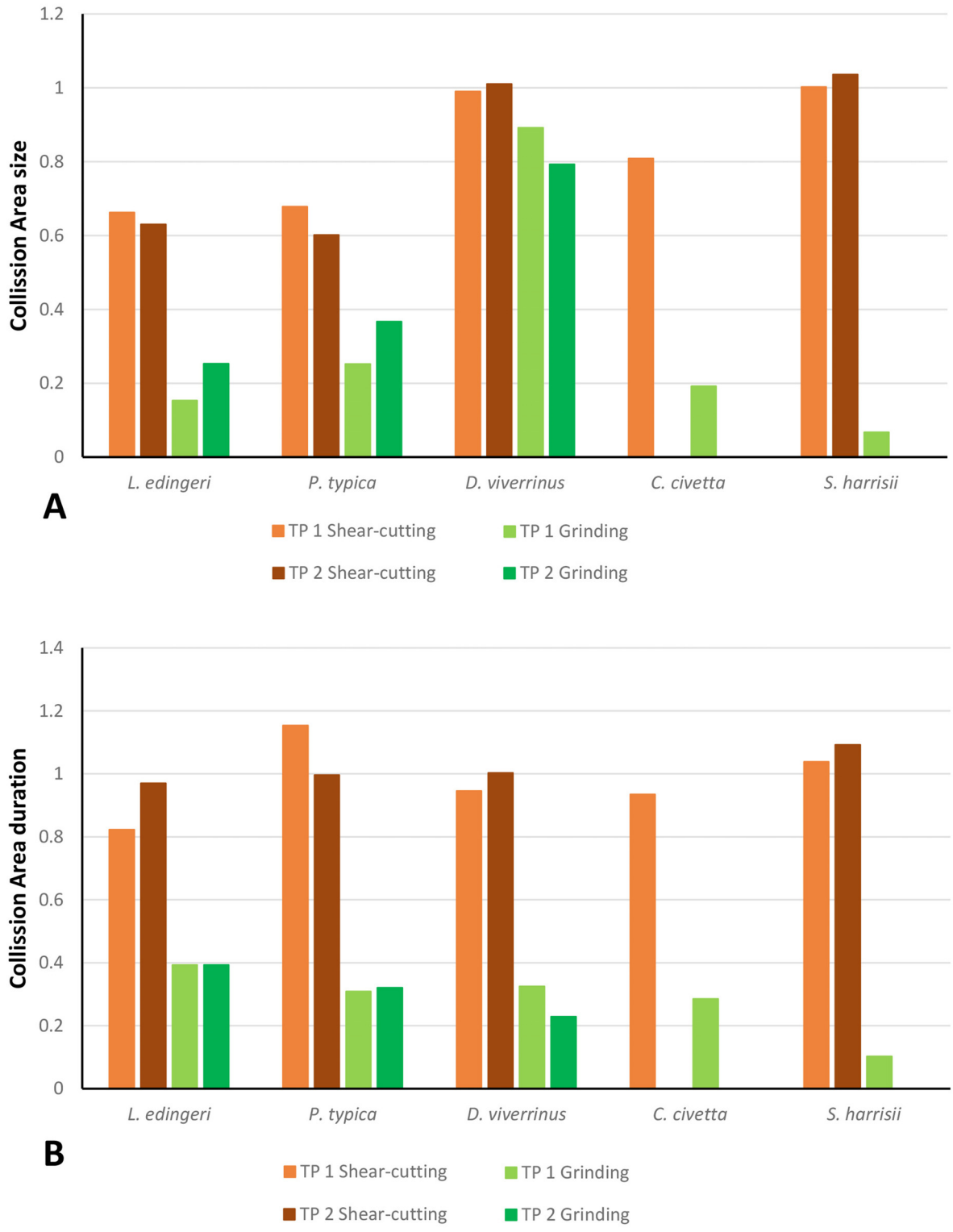

FIGURE 12. Combined values for single molar (A) Collision Area (CA) size and (B) Collision Area duration divided by their function. TP 1 marks the first lower molar in each complex, while TP 2 marks the second lower molar. Percentages for each Collision Area are added up and can therefore exceed the 100%.

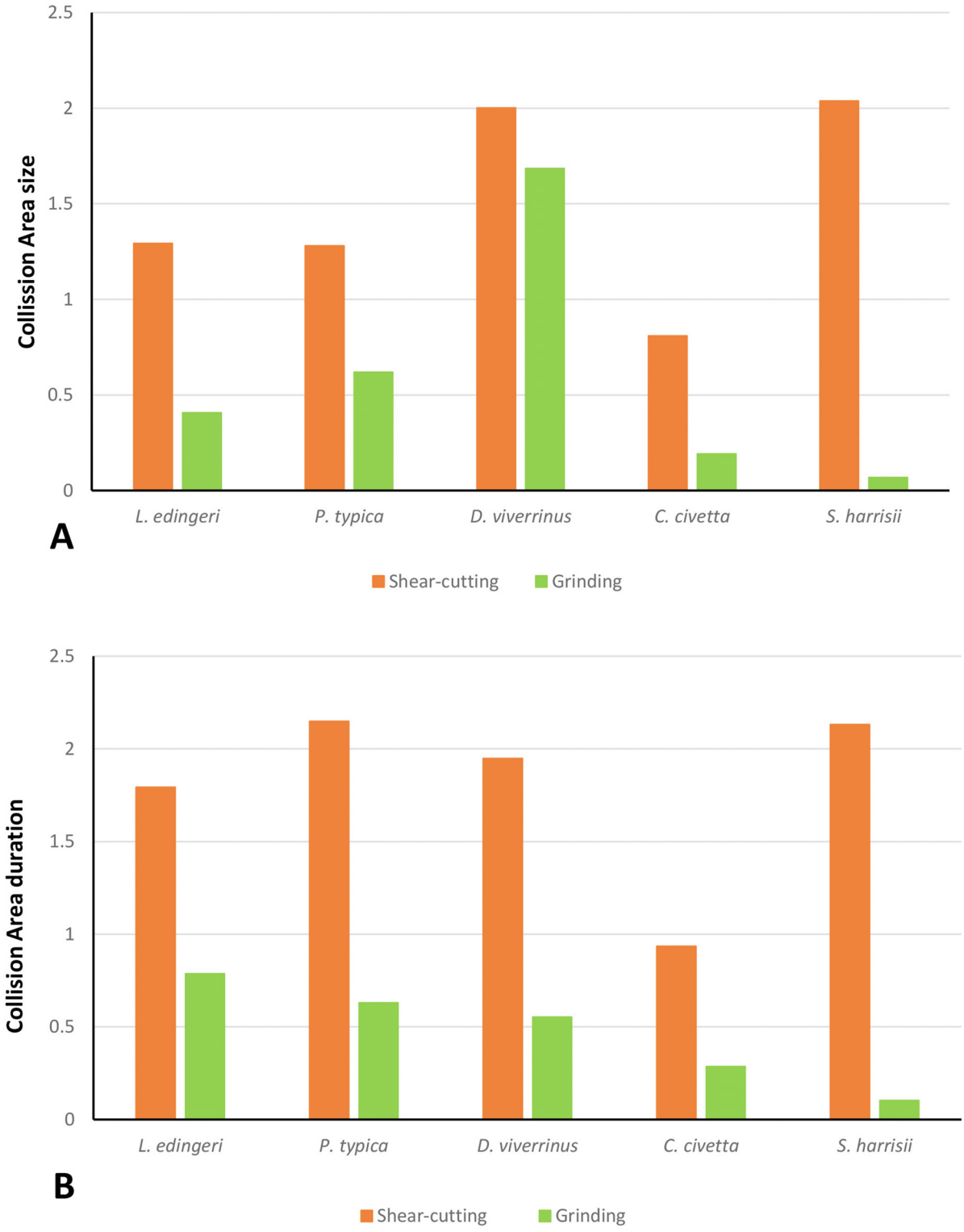

FIGURE 13. Combined values for both molars. Showing (A) Collision Area (CA) size and (B) Collision Area duration divided into their function. Percentages for each CA are combined and can therefore exceed 100%.

The highly reduced talonid basin in *Sarcophilus harrisii* offers only a small surface for the likewise reduced protocone (Solé and Mennecart 2019). A small collision area (CA 3) is therefore not surprising (Figures 10-13). Early in the chewing cycle, the large size and long collision duration of CA 1 and CA 2 show that the main function lies in the blades for the shear-cutting function for a highly carnivorous diet (Stannard et al., 2017). In addition, collision duration and size of CA 1 are somewhat longer and larger than in CA 2, underlining the emphasis on the paracristid as the main cutting edge (Figure 11).

In *Civettictis civetta* facets of the talonid basin identified with the help of high detail epoxy resin casts revealed a difference to the facets identified in the carnassials. Instead of smooth and light-reflecting surfaces that show striations caused by attrition like in the carnassials, the hypoconid and entoconid and the hypoconulid of *C. civetta* are rounded and appear duller when exposed to light, suggesting that tooth wear is caused primarily by abrasion instead of attrition. This usually occurs when tooth substance is worn down by tooth-to-food contact rather than tooth-to-tooth contact (Grippo et al., 2004; López-Frías et al., 2012).

An open morphology (i.e., low cusps and crests bordering the talonid basin) and levelled relief of the molars in general (i.e., lower cusp height, lower crown base) compared with the other taxa gives little space for CA 2 to build up, making differentiation between CA 2 and CA 3 difficult and points toward softer food sources. Similar tooth morphologies can be observed, for example in primates with low relief in molars and increased tooth-to-food contact (Rosenberger and Kinzey, 1976; Norconk, 1996). The diet of *C. civetta* consists of fruits and berries over long periods of time during the year and shifts to a more meat and insect-based nutrition in the dry season (Bekele et al., 2008; Mullu and Balakrishnan, 2014) underlining the necessity for fully functional carnassials. Because of this more meat-based nutrition in dry season, abrasion would play, during that time, a minor role in the dentition. Additionally, since the presence of food cannot be simulated within the OFA simulation, the program is more suited for showing the specific circumstance of tooth-to-tooth contact, rather than tooth-to-food contact. Consequently, tooth-to-food contact in *C. civetta* could result in an apparently reduced contact of the individual teeth in the OFA simulation. In turn, this would result in the overrepresentation of CA 1 and CA 2, but an underrepresentation of CA 3 due to the limits of the program used. This becomes especially visible in TP 2 for *C. civetta* in which the involved teeth show no carnassial-like structures and a very low morphological relief of the teeth. Combined with dull reflections from the above-mentioned epoxy resin casts, this leads to the conclusion that mainly abrasion takes place at TP 2 and hardly any collisions areas can be detected by the OFA.

The process of mechanical grinding within the talonid basin seems to be more important in the chewing cycle of the marsupial *D. viverrinus* when compared to *L. edingeri* and *P. typica*. *Dasyurus viverrinus* in general shows a quite varied diet. One main part of its nutrition is provided by plants consisting of grass leaves, seeds and other plant material (Blackhall, 1980). Grass is consumed throughout the year in small amounts (Jones and Rose, 2001). The other important food source during the year are insects. Vertebrates like small mammals and birds are consumed to a lesser degree by *D. viverrinus* (Blackhall, 1980; Jones and Rose, 2001; Francourt et al., 2018; Shippley et al., 2025).

Research on demands in shearing and crushing in an insectivorous diet showed that long lasting shearing facets with relatively large and long-lasting occlusal surfaces or morphological structures like the carnassials, are well-suited for soft bodied insects (Strait, 1993; Ungar, 2010). While a long blade would provide sufficient surface to cut through a food item, the carnassial structure would keep it trapped, preventing it from escaping. Hard bodied insects, like beetles, would demand more focused pressures and therefore slender cusps to break the cuticle (Strait, 1993; Evans and Sanson, 2006; Ungar, 2010). Following this, the CEI should be consequently high for tough food that is harder to cut through and small for hard and rigid bodied food items.

High shares in grinding function of CA 3 as detected in the chewing cycle of *D. viverrinus* can be interpreted because of the constant ingestion and processing of plant matter over the year. *Lesmesodon edingeri* and *P. typica* do not show an emphasis on CA 3 function. Shear-cutting in *Dasyurus viverrinus* is distributed somewhat equally over CA 1 and CA 2 despite size and duration differences between the TPs. The distribution of collision areas is comparable to those of *L. edingeri*, but *P. typica* has a higher collision duration, indicating a possible emphasis on softer prey (Figures 12, 13). *Proviverra typica* matches in the collision duration with *S. harrisii* indicating that a

heavily meat-based diet results in similar CA duration. CA size in *P. typica* is lower, indicating adaptations for piercing harder bodied prey, while *S. harrisii* shows, as already mentioned earlier, the highest CA sizes of the range.

Concerning both CEIs (active and complete) (Tables 3 and 4), the rather short cutting edges of *L. edingeri* suggest a preference for harder food items. In comparison *P. typica* and *D. viverrinus* show mixed signals in the CEIs. The high CEIs in the upper molars of *P. typica* suggest a preference of soft bodied insects in the diet, while the CEIs of the lower molars are comparable to those of *L. edingeri* which suggest a diet consisting of more hard bodied prey. In case of *D. viverrinus* it is the opposite situation, with lower CEIs in the upper and comparatively high CEIs in the lower molars.

Sarcophilus harrisii has generally high CEIs, which again suggests that meat is processed in the same way as soft bodied insects (i.e., larvae and moths), since *S. harrisii* is known to be hypercarnivorous (Pemberton et al., 2008; Bell et al., 2021). It is important to mention, that *S. harrisii* is also known to actively chew and process bones of carcasses up to the size of wombats (*Vombatus ursinus*) (Jones, 1996; Pollock, 2021). Accordingly, the dietary adaptation of the Tasmanian devil is also classified as durophagous (Reside and Desantis, 2022; Warburton et al., 2024;). However, tooth wear caused through processing of bones occurs mainly on the canine and M2 (Pollock, 2021; Jones, 2023). Jones (1996) misidentified the M2 as M3, by following the interpretation of the tooth formula by Archer (1978) (M2-M5). According to today´s todays dental formula for *Dasyuridae*, the tooth in question is the M2. Jones (1996) also stated: *"Instead, the second molar, classified as M3 by Archer (1978), and to a lesser extent M2, are used for bone-crushing and are worn to stumps in old animals."* The "M2" of Jones (1996) is the M1 according to current interpretation (Pollock, 2021; Jones, 2023) and the mentioned M3 is the actual M2.

Furthermore, Jones (1996) mentions the "toughness" of skin of bigger prey such as wombats (*Vombatus ursinus*), which have been reported to actively be preyed and consumed by *S. harrisii* (Andersen et al., 2017). A study on microwear of Tasmanian devils observed no functional difference between molar tooth positions (Jiang and deSantis, 2014), suggesting that all molars (i.e., M1-M4) of *S. harrisii* are suited for chewing bone, but also for working through tough skin. While canine, M1, and M2 are mainly used for chewing through bones which causes strong wear, the much less worn M3 and M4 keep being suited for working through tough materials.

Dasyurus viverrinus feeds on small mammals as well as birds (Blackhall, 1980; Jones and Rose, 2001). The insect part of *D. viverrinus* nutrition consists mainly of soft-bodied larvae. The predominant diet composition for *D. viverrinus* justify the relatively long duration and the large size of CA 1 and CA 2, which are better suited for processing meat and soft bodied insects, whereas those of CA 3 can be attributed to the steady processing of plant material over the year.

Morlo and Habersetzer (1999) described the diet of *L. edingeri* as mainly carnivorous with insects being a regular part of it. The results of the OFA analysis of *L. edingeri* would support this hypothesis and would still be compatible with the gut content findings of smaller vertebrates (Morlo et al., 2011; Gunnel et al., 2018). CA 3 shows a lower demand for grinding function, indicating that *L. edingeri* did not process plant material to the level of *D. viverrinus*. We wish, however, to emphasize that the overall lower CEIs of *L. edingeri* (Tables 3 and 4) could be ontogenetically influenced, as the investigated individual (HLMD-Me 14590a) is a juvenile.

The size of shear-cutting function CAs of the juvenile *L. edingeri* matches with those of *P. typica.* Duration is slightly higher in *P. typica* but still suggests that the dentition is adapted to dietary resources similar to *D. viverrinus*. To the best of our knowledge, stomach contents of *P. typica* are hitherto unknown. Being only slightly smaller than *L. edingeri*, *P. typica* is suspected to have had a similar diet (Morlo and Habersetzer, 1999).

Small CA size, as mentioned above, suggests a focus on harder bodied food sources in general as the higher relative pressures would have been suited for driving cracks easier into e.g., the hard/brittle cuticle of an insect's body. Small cutting edges might indicate adaptations for harder food sources as well as enabling the appliance of higher stresses onto a relatively small area of the food item (Strait, 1993; Evans and Sanson, 2006; Ungar, 2010).

CEIs in *L. edingeri* give a mixed signal. Lower molar CEI appears to be on the lower end of the range and would support an adaptation towards harder bodied food material. In contrast, upper molar CEIs and CA durations fall within the range of *D. viverrinus* and suggest an adaptation for softer bodied prey. *Proviverra typica* appears to be comparable to *L. edingeri* in CAs but shows higher

CEIs and therefore seems to be more adapted towards softer bodied prey than *L. edingeri*. Longer CA durations can however also be necessary to maintain pressure and drive cracks further through the prey to process it to a higher degree (Strait, 1993; Ungar, 2010).

CA 3 has a relatively higher share in size in *P. typica* than in *L. edingeri*. Ungar (2010) suggested that species with low tooth crown relief (i.e., higher shares in crushing CAs), tend to feed more likely on harder food. The duration of this CA is however lower in *P. typica* compared to *L. edingeri* and closer to the one of *D. viverrinus*. Since no gut content of *P. typica* has been found so far, we cannot recognize a tendency towards harder or softer bodied food material as shares in duration and size seem to level each other out between *L. edingeri* and *P. typica*.

The higher shares seen in *Dasyurus viverrinus* in grinding are probably due to the steady processing of plant material, as has been reported for the species (Blackhall, 1980; Jones and Rose, 2001).

Concerning *Lesmesodon edingeri* and *Proviverra typica*, it seems that the dentition of *L. edingeri* would have been more suited for processing harder bodied food material compared to *P. typica*. The differences in CA shares are however, small and cannot be considered significant. Only the CEIs appear to be more different. As a result, we come to a similar conclusion as Morlo and Habersetzer (1999) and suggest a comparable diet for *Lesmesodon edingeri* and *Proviverra typica* based on the distribution of CA durations and sizes between these two fossil taxa. It should be kept in mind, however, that an adult specimen of *P. typica* is compared with a juvenile or subadult individual of *L. edingeri*. It remains unclear for now how much the ontogenetic stage influences the shares in CA and the size in CEI.

Chewing Cycle

In general chewing cycle length is influenced by body size and ontogenetic development. Older individuals and larger species tend to have longer chewing cycles (Gerstner and Gerstein, 2008; Stover and Williams, 2011). This also seems to apply to the insectivorous taxa analyzed. *Dasyurus viverrinus,* with an estimated body weight of up to 1.1 kg (Jones and Rose, 2001), is slightly larger than *Lesmesodon edingeri* and *Proviverra typica* (both estimated at < 1 kg) (Morlo and Habersetzer, 1999) and shows a slightly longer reconstructed chewing cycle. Following this, the chewing cycle of *Sarcophilus harrisii* (body weight = 9 kg according to Rose et al., 2017) should however be shorter than for *Civettictis civetta* with 15-20 kg (Ray, 1995). The low rise in slope in *S. harrisii* and *C. civetta* (Figure 4) shows that the amount of tooth surface that has actual tooth-to-tooth contact in relationship to the total tooth surface is relatively small. The high shares of shear-cutting (CA 1 and CA 2) on relatively small occlusal surfaces point to a high efficiency within this function in *S. harrisii*. Analysis of carnivorous dentitions by Evans and Fortelius (2008) showed that this is characteristic for teeth, where convex blades collide with each other, maintaining their contact until the end of the power stroke and keeping the cutting function as efficient as possible. Therefore, the long collision times of the shear-cutting CAs, which can be accounted for by many of all collisions taking place, provide a high efficiency in dealing with tough food. In *C. civetta*, the shear-cutting efficiency seems to be less pronounced than in *S. harrisii* since CAs 1 and 2 have lower shares in terms of size than in *S. harrisii*, while duration is not too far off (Figures 10-13). It is also important to note that only the CA 1 and 2 of TP 1 could be considered. CA 2 has higher shares in size than CA 1 in *C. civetta* which is consistent with what we see in the chewing cycle (Figure 4, see *4) where, as discussed below, the transition phase shows the highest collision in the complex.

The initial rise in slope in all species can be accounted to either CA 1 or CA 2 where food/prey gets fixated, punctured, cut and sheared apart. In *Sarcophilus harrisii* CA 1 marks the highest occlusal contact (Figure 4, see *3), showing that the shear-cutting function is most important for this species. The decline shows at which point the main part of the shearing blades passed each other. The dentition of *C. civetta* shows the direct opposite. CA 1 has little effect, while CA 2 is responsible for the highest rise (Figure 4, see *2). Initially also functioning for shear-cutting, M1 relatively soon occludes into the talonid basin, forming CA 3 and gradually adding more grinding and crushing function as the colliding surfaces become continually more horizontal with progressing occlusion. With the highest amount of collision observed in this transitional step (Figure 4, see *4), it suggests that this is the most important function in the dentition of *C. civetta*.

Shear-cutting function in all insectivorous species from this study is responsible for the first ascent in the graphs, irrespective of which CA (i.e., CA 1 or CA 2) builds the first occlusions. In no spe-

cies, however, they are responsible for the maximum collision alone. The highest amount of collision results always from a combination of parts of all three here analyzed CAs together (Figure 4). This supports the assumption that the initial occlusion of the protocone into the talonid basin and the associated grinding is playing an important role in the masticatory path. The minor importance of CA 3 in *S. harrisii* can be interpreted in the same manner, as it is found at the point of lowest surface collision throughout the cycle. Phase II is marked in all species with a steady decrease in surface collision due to the decrease of colliding occlusal surfaces with the ending of CA 1 and CA 2 and the decoupling of the structures.

Ecological Implications

To understand the ecological role of fossil taxa, knowledge about their feeding behavior is crucial. Reconstruction of the diet of extinct taxa is difficult and can often only be achieved by comparing the preserved dentitions and cranial characters with those of morphologically similar extant species (van Valkenburgh, 1988; Witmer and Rose, 1991; Morlo, 2004). It must be kept in mind, however, that phylogenetic distance can have an impact on the interpretation and nuance the application of the uniformitarianism principle (Scott, 1963; Tiffney, 2008; Erwin, 2011; Lyman, 2017).

Like *Dasyurus viverrinus*, the small hyaenodonts are described as predominantly terrestrial, hunting on the ground when reaching adulthood (MacLeod and Rose, 1993; Morlo and Habersetzer, 1999; Jones and Rose, 2001).

Superficially, the morphology of the dentition is most similar between *Dasyurus viverrinus*, *Lesmesodon edingeri*, and *Proviverra typica*, and despite some variation, shares for shear-cutting in between CA 1 and CA 2 are comparable. This implies similar adaptations for carnivorous/insectivorous diet which is supported by the analysis presented here. The dentitions of *L. edingeri* and *P. typica* compared to *D. viverrinus* seem similar in adaption to soft bodied insects (i.e., worms or insect larvae), and for processing meat. The analysis of the collision areas and wear facets complemented by the comparison of the *Dasyurus viverrinus* diet and the known preserved stomach contents from *L. edingeri* allow for a more exact picture of the lifestyle of *Lesmesodon edingeri*.

Insect larvae are an important food source and are consumed all year by *D. viverrinus*. Insects are also among the most abundant fossils preserved in the Messel Pit with all major groups present (Smith et al., 2018, 2024) suggesting that insect larvae were a viable food source for *L. edingeri* (and by extrapolation for *P. typica)* all around the year.

Small vertebrates are very common in the Messel fossillagerstätte as well (Smith et al., 2024), and we have direct proof (i.e., stomach content) that at least one individual of *L. edingeri* consumed such prey while the deciduous dentition was still present (Morlo and Habersetzer, 1999; Gunnell et al., 2018).

Dasyurus viverrinus have been reported to prey on animals up to the size of domestic chickens (Blackhall, 1980; Jones and Rose, 2001). The most abundant tetrapod group in the fossil record of Messel are birds (see Smith et al., 2024). A very common Messel fossil bird, *Messelornis cristata* (~25 cm in height), which was presumably ground-nesting (Morlo, 2004; Mayr, 2017) and smaller than domestic chickens, could have been a possible food source at least for *Lesmesodon edingeri.*

It is also worth mentioning that scavenging is common behavior for carnivores (Kane et al., 2017). Since this behavior has been reported for *D. viverrinus*, it is not unlikely that *L. edingeri* and *P. typica* did scavenge from time to time as well. As swift small-bodied ground hunters, they could have scurried around carcasses of larger prey, snatching off their share of the meat (Morlo and Habersetzter, 1999). However, direct evidence for scavenging is not given by our analysis and can only be suggested by its adaptions for soft-bodied food sources and extrapolated from the behavior of extant *D. viverrinus.*

Lesmesodon edingeri is only known from the Messel Pit, dated from the early middle Eocene (MP 11) (Solé et al. 2021), which experienced a "greenhouse climate" with CO_2 concentration and average air temperature higher than in today's Europe (Tütken, 2014). In comparison, *D. viverrinus* is endemic to more maritime climates, mainly under the influence of oceanic climate cycles. The ecosystem in which *L. edingeri* lived was less affected by seasonality and mean temperature was ~5° higher than in the natural habitat of *D. viverrinus* today, although the conditions at the Messel locality were getting dryer in later stages (Grose et al., 2010; Tütken, 2014; Lenz et al., 2011; Kaboth-Bahr et al., 2024).

With less pronounced seasonality in the habitat of *L. edingeri,* adaptations to seasonal food changes would have been less necessary. Therefore, an adaptation to a wider food range, such as the seasonal intake of fruits, different insects and

vertebrates observed in *D. viverrinus* (e.g., Jones and Rose, 2001; Fancourt et al., 2018; Shippley et al., 2025), is less likely. To investigate the patterning in occlusal dynamics in future studies of comparable extant and extinct mammal groups (representatives of e.g., dasyurids, didelphids, erinaceids), dietary effects based on seasonality should be taken into consideration.

CONCLUSION

The goal of this study was to reconstruct and compare the dentition and chewing cycle of the hyaenodont *Lesmesodon edingeri* with that of extant carnivores with known diet and different tooth morphologies to functionally classify the dentition and to get new insights about the feeding type and lifestyle of this fossil species. With the help of the OFA, it was possible to analyze CAs of a fossil individual and compare it with a range of feeding types from omnivorous to hypercarnivorous diets as well as with other fossil taxa. We showed that *L. edingeri* has similarities in tooth function with other extinct close relatives (i.e., *P. typica*), and with extant insectivorous species. It was demonstrated that differences in the chewing cycles occur between *L. edingeri, P. typica,* and *D. viverrinus* despite the quite similar carnassial morphology, even though they are not visible on a macroscopic scale.

The results presented here add to our understanding of the ecology of *L. edingeri*. The results support previous suggestions about its diet and new assumptions on preferred prey are possible. Since the Messel Pit is a well-known fossil site that is subject to extensive scientific studies and has a rich fossil record, this study contributes to the overall picture of an Eocene fauna by highlighting possible hunter-prey relationships.

The CA analysis allowed an evaluation of the ecology of closely related extinct species and highlighted the differences in their diets. In that respect, *P. typica*, as a close relative of *L. edingeri* (after Dubied et al., 2019; Solé and Mennecart, 2019) probably had a diet similar to that of *L. edingeri*.

ACKNOWLEDGEMENTS

We would like to thank all the institutions involved for providing the objects used in this study. We would also like to thank the paleontology department of the Natural History Museum in Karlsruhe for giving us the opportunity to finish this manuscript in their working group.

REFERENCES

Andersen, G.E., Johnson, C.N., Barmuta, L.A., and Jones, M.E. 2017. Dietary partitioning of Australia's two marsupial hypercarnivores, the Tasmanian devil and the spotted-tailed quoll, across their shared distributional range. PLoS ONE 12 (11):e0188529. https://doi.org/10.1371/journal. pone.0188529

Ackermann, M., Habersetzer, J., and Schaarschmidt, F. 1988. Von der Ausgrabung zum Ausstellungsstück, p. 279–284. In Schaal, S. and Ziegler, W. (eds.), Messel - Ein Schaufenster in die Geschichte der Erde und des Lebens, Verlag Waldemar Kramer, Frankfurt am Main.

Ackermans, N. L., Winkler, D.E., Schulz-Kornas, E., Kaiser, T.M., Müller, D.W.H., Kircher, P.R., Hummel, J., Clauss, M., and Hatt, J.-M. 2018. Controlled feeding experiments with diets of different abrasiveness reveal slow development of mesowear signal in goats *(Capra aegagrus hircus).* The Journal of experimental biology 221 (21). https://doi.org/10.1242/jeb.186411

Archer, M. 1978. The nature of the molar-premolar boundary in marsupials and a reinterpretation of the homology of marsupial cheekteeth. Memoirs of the Queensland Museum, 18:157–164.

Archer, M., Flannery, T.F., Ritchie, A., and Molnar, R.E. 1985. First Mesozoic mammal from Australia—an early Cretaceous monotreme. Nature 318:363–366. https://doi.org/10.1038/318363a0

Barry, J.C. 1988. *Dissopsalis*, a middle and late Miocene proviverrine creodont (Mammalia) from Pakistan and Kenya. Journal of Vertebrate Paleontology, 8:25–45. https://doi.org/10.1080/02724634.1988.10011682

Bastl, K., Morlo, M., Nagel, D., and Heizmann, E. 2011. Differences in the tooth eruption sequence in *Hyaenodon* ('Creodonta': Mammalia) and implications for the systematics of the

genus. Journal of Vertebrate Paleontology, 31:181–192. https://doi.org/10.1080/02724634.2011.540052

Bastl, K. and Nagel, D. 2014. First evidence of the tooth eruption sequence of the upper jaw in *Hyaenodon* (Hyaenodontidae, Mammalia) and new information on the ontogenetic development of its dentition. Paläontologische Zeitschrift, 88:481–494. https://doi.org/10.1007/s12542-013-0207-z

Bekele, T., Afework, B., and Balakrishnan, M. 2008. Scent-marking by the African Civet *Civettictis civetta* in the Menagesha– Suba State Forest, Ethiopia. Small Carnivore Conservation, 38:29–33.

Bell, O., Jones, Menna E., Ruiz A., Manuel; H.-R., Rodrigo K., Bearhop, S., and McDonald, R.A. 2021. Data from: Age-related variation in the trophic characteristics of a marsupial carnivore, the Tasmanian devil *Sarcophilus harrisii*. Dryad. https://doi.org/10.5061/dryad.m905qftz8

Bi, S., Zheng, X., Wang, X., Cignetti, N.E., Yang, S., and Wible, J.R. 2018. An Early Cretaceous eutherian and the placental-marsupial dichotomy. Nature, 558:390–395. https://doi.org/10.1038/s41586-018-0210-3

Black, K.H., Archer, M., Hand, S.J., and Godthelp, H. 2010. First comprehensive analysis of cranial ontogeny in a fossil marsupial—from a 15-million-year-old cave deposit in northern Australia. Journal of Vertebrate Paleontology, 30:993–1011. https://doi.org/10.1080/02724634.2010.483567

Blackhall, S. 1980. Diet of the Eastern Native-Cat, *Dasyurus viverrinus* (Shaw), in Southern Tasmania. Australian Wildlife Research, 7:191–197. https://doi.org/10.1071/WR9800191

Borths, M.R. and Stevens, N.J. 2019. *Simbakubwa kutokaafrika*, gen. et sp. nov. (Hyainailourinae, Hyaenodonta, 'Creodonta,' Mammalia), a gigantic carnivore from the earliest Miocene of Kenya. Journal of Vertebrate Paleontology, 39:e1570222. https://doi.org/10.1080/02724634.2019.1570222

Borths, M.R. and Stevens, N.J. 2017. The first hyaenodont from the late Oligocene Nsungwe Formation of Tanzania: Paleoecological insights into the Paleogene-Neogene carnivore transition. PLoS ONE, 12(10):e0185301. https://doi.org/10.1371/journal.pone.0185301

Davis, B.M. 2011. Evolution of the tribosphenic molar pattern in early mammals, with comments on the "dual-origin" hypothesis. Journal of Mammalian Evolution, 18:227–244. https://doi.org/10.1007/s10914-011-9168-8

DeSantis, L.R.G. 2016. Dental microwear textures: reconstructing diets of fossil mammals. Surface Topography: Metrology and Properties, 4:S.23002. https://doi.org/10.1088/2051-672x/4/2/023002

Dubied, M., Solé, F., and Mennecart, B. 2019. The cranium of *Proviverra typica* (Mammalia, Hyaenodonta) and its impact on hyaenodont phylogeny and endocranial evolution. Palaeontology, 62:983–1001. https://doi.org/10.1111/pala.12437

Egi, N., Holroyd, P. A., Tsubamoto, T., Soe, A. N., Takai, M., and Ciochon, R. L. 2005. Proviverrine hyaenodontids (Creodonta: Mammalia) from the Eocene of Myanmar and a phylogenetic analysis of the proviverrines from the Para?Tethys area. Journal of Systematic Palaeontology, 3:337–358. https://doi.org/10.1017/S1477201905001707

Engels, S. and Schultz, J.A. 2019. Evolution of the power stroke in early Equoidea (Perissodactyla, Mammalia). Palaeobiodiversity and Palaeoenvironments, 99:271–291. https://doi.org/10.1007/s12549-018-0341-4

Erwin, D.H. 2011. Evolutionary uniformitarianism. Developmental Biology, 357:27–34. https://doi.org/10.1016/j.ydbio.2011.01.020

Evans, A.R. and Sanson G.D. 2006. Spatial and functional modeling of carnivore and insectivore molariform teeth. Journal of Morphology, 267:649–662. https://doi.org/10.1002/jmor.10285

Evans, A.R. and Fortelius, Mikael. 2008. Three-dimensional reconstruction of tooth relationships during carnivoran chewing. Palaeontologia Electronica, 11.2.10A:1–11. https://palaeo-electronica.org/2008_2/133/index.html

Fancourt, B.A., Hawkins, C.E., and Nicol, S.C. 2018. Mechanisms of climate-change-induced species decline: spatial, temporal and long-term variation in the diet of an endangered

marsupial carnivore, the eastern quoll. Wildlife Research, 45:737–750. https://doi.org/10.1071/WR18063

Flynn, J.J., Finarelli J.A., and Spaulding, M. 2010. Phylogeny of the Carnivora and Carnivoramorpha, and the use of the fossil record to enhance understanding of evolutionary transformations. Carnivoran Evolution, p.25–63. In Goswami, A. and Friscia A. (eds.), Carnivoran Evolution: New Views on Phylogeny, Form and Function, Cambridge University Press, Cambridge. https://doi.org/10.1017/CBO9781139193436.003

Fortelius, M. and Solounias, N. 2000. Functional Characterization of Ungulate Molars Using the Abrasion-Attrition Wear Gradient: A New Method for Reconstructing Paleodiets. American Museum Novitates 2000:1-36. https://doi.org/10.1206/0003-0082(2000)301<0001:FCOUMU>2.0.CO;2

Fraser, G.J. and Hulsey, C.D. 2020. Biology at the Cusp: Teeth as a Model Phenotype for Integrating Developmental Genomics, Biomechanics, and Ecology. Integrative and Comparative Biology, 60:559–562. https://doi.org/10.1093/icb/icaa104

Frederickson, J., Cohen, J., Engel, M., Hunt, T., Wilbert, G., Castañeda, O., and Czaplewski, N. 2022. The paleoecology of the Late Miocene mammals from the Optima Local Fauna of Oklahoma, USA. Acta Palaeontologica Polonica, 67:221–238. https://doi.org/10.4202/app.00941.2021

Gagnot, G., Yardin, M., Delevaux, F., and Hernanie, C. 1977. Sur le développement musculo - aponévrotique du muscle masseter du lapin *(Oryctolagus cuniculus).* Mammalia, 41:529–536. https://doi.org/10.1515/mamm.1977.41.4.529

Gerstner, G.E. and Gerstein, J.B. 2008. Chewing Rate Allometry Among Mammals. Journal of Mammalogy, 89:1020–1030. https://doi.org/10.1644/07-MAMM-A-188.1

Gheerbrant, E., Iarochene, M., Amaghzaz, M., and Bouya, B. 2006. Early African hyaenodontid mammals and their bearing on the origin of the Creodonta. Geological Magazine, 143:475–489. https://doi.org/10.1017/S0016756806002032

Goswami, A., Milne, N., and Wroe, S. 2011. Biting through constraints: cranial morphology, disparity and convergence across living and fossil carnivorous mammals. Proceedings of the Royal Society B, 278:1831–1839. https://doi.org/10.1098/rspb.2010.2031

Grippo, J.O., Simring, M., and Schreiner, S. 2004. Attrition, abrasion, corrosion and abfraction revisited: a new perspective on tooth surface lesions. Journal of the American Dental Association, 135:1109–1118. https://doi.org/10.14219/jada.archive.2004.0369

Grose, M.R., Barnes-Keoghan, I., Corney, S.P., White C.J., Holz, G.K., Bennett, J.B., Gaynor, S.M., and Bindoff, N.L. 2010. Climate Futures for Tasmania: general climate impacts technical report. Antarctic Climate & Ecosystems Cooperative Research Centre, Hobart.

Gunnell, G.F., Lehmann, T., Ruf, I., Habersetzer, J., Morlo, M., and Rose, K.D. 2018. Ferae: animals that eat animals. In K. T. Smith, S. F. K. Schaal, & J. Habersetzer (Eds.), Messel-An Ancient Greenhouse Ecosystem 271–294, Schweizerbart, Stuttgart.

Habtamu, T., Bekele, A., Ahmed, R., Gadisa, T., Birlie, B., Tolemariam, T., and Belay, B. 2017. Diets of the African Civet *Civettictis civetta* (Schreber, 1778) in selected coffee forest habitat, south-western Ethiopia. African Journal of Ecology, 55:573–579. https://doi.org/10.1111/aje.12390

Halliday, T.J.D., Upchurch, P., and Goswami, A. 2017. Resolving the relationships of Paleocene placental mammals. Biological reviews of the Cambridge Philosophical Society, 92:521–550. https://doi.org/10.1111/brv.12242

Hiiemae, K.M. and Kay, R.F. 1972. Trends in the evolution of primate mastication. Nature, 240:486–487. https://doi.org/10.1038/240486a0

Hiiemae, K.M. and Kay, R.F. 1973. Evolutionary trends in the dynamics of Primate mastication, In Zingeser, M.R. (ed.), Symposia of the 4. International congress of primatology Craniofacial Biology of Primates 3:28–64, Karger Publishers, Basel.

Jäger, K.R.K., Cifelli, R.L., and Martin, T. 2020. Molar occlusion and jaw roll in early crown mammals. Scientific reports, 10:S.22378. https://doi.org/10.1038/s41598-020-79159-4

Jäger, K.R.K., Gill, P.G., Corfe, I., and Martin, T. 2019. Occlusion and dental function of *Morganucodon* and *Megazostrodon*. Journal of Vertebrate Paleontology, 39:e1635135. https://doi.org/10.1080/02724634.2019.1635135

Jiang, T. and DeSantis, L.R. 2014. Dental microwear texture analysis of the tasmanian devil: assessing variability among teeth. Young Scientist, 4:30–32.

Jones, M. 1996. Guild structure of the large marsupial carnivores in Tasmania. PhD Thesis, University of Tasmania, Hobart, Australia. https://doi.org/10.25959/23211611.v1

Jones M.E. 2023 Over-eruption in marsupial carnivore teeth: compensation for a constraint. Proceedings of the Royal Society Publishing B. 290:20230644. https://doi.org/10.1098/rspb.2023.0644

Jones, M.E. and Rose, R.K. 2001. *Dasyurus viverrinus*. Mammalian Species, 677:1–9. https://doi.org/10.1644/1545-1410(2001)677<0001:DV>2.0.CO;2

Kaboth-Bahr, S., Schmitt, C., Bauersachs, T., Zeeden, C., Wonik, T., Schandl, J., Lenz, O., Wedmann, S., Vasiliev, I., Mulch, A.,; Lourens, L., Pross, J., and Bahr, A. 2024. Improved chronostratigraphy for the Messel Formation (Hesse, Germany) provides insight into early to middle Eocene climate variability. Newsletters on Stratigraphy, 57:153–170. https://doi.org/10.1127/nos/2024/0799

Kane, A., Healy, K., Guillerme, T., Ruxton, G.D., and Jackson, A.L. 2017. A recipe for scavenging in vertebrates - the natural history of a behaviour. Ecography, 40:324–334. https://doi.org/10.1111/ecog.02817

Koenigswald, W.v. 2018. Specialized wear facets and late ontogeny in mammalian dentitions, Historical Biology, 30:1–2, 7—29. https://doi.org/10.1080/08912963.2016.1256399

Kühne, W.G. 1962. Präparation von flachen Wirbeltierfossilien aus kolloidalem Gestein. Paläontologische Zeitschrift, 36:285–286. https://doi.org/10.1007/BF02986981

Kullmer, O., Benazzi, S., Fiorenza, L., Schulz., Bacso, S., and Winzen, O. 2009. Technical note: Occlusal fingerprint analysis: quantification of tooth wear pattern. American Journal of Physical Anthropology, 139:600–605. https://doi.org/10.1002/ajpa.21086

Lange-Badré, B. 1979. Les Créodontes (Mammalia) d'Europe occidentale de l'Éocène supérieur à l'Oligocène supérieur. Mémoires du Muséum national d'Histoire naturelle, série C, 42: 1–249.

Lenz, O.K., Wilde, V., and Riegel, W. 2011. Short-term fluctuations in vegetation and phytoplankton during the Middle Eocene greenhouse climate: a 640-kyr record from the Messel oil shale (Germany). International Journal of Earth Sciences, 100:1851–1874. https://doi.org/10.1007/s00531-010-0609-z

Leonard, K.C., Boettcher, M.L., Dickinson, E., Malhotra, N., Aujard, F., Herrel, A., and Hartstone-Rose, A. 2020. The Ontogeny of Masticatory Muscle Architecture in *Microcebus murinus.* The Anatomical record, 303:1364–1373. https://doi.org/10.1002/ar.24259

López-Frías, F.J., Castellanos-Cosano, L., Martín-González, J., Llamas-Carreras, J.M.,, and Segura-Egea, J.J. 2012. Clinical measurement of tooth wear: Tooth wear indices. Journal of clinical and experimental dentistry, 4:e48-53. https://doi.org/10.4317/jced.50592

Luo, Z.-X., Cifelli, R.L., and Kielan-Jaworowska, Z. 2001. Dual origin of tribosphenic mammals. Nature 409:53–57. https://doi.org/10.1038/35051023

Luo, Z.-X., Ji, Q., and Yuan, C.-X. 2007. Convergent dental adaptations in pseudo-tribosphenic and tribosphenic mammals. Nature, 450:93–97. https://doi.org/10.1038/nature06221

Luo, Z.-X., Yuan, C.-X., Meng, Q.-J., and Ji, Q. 2011. A Jurassic eutherian mammal and divergence of marsupials and placentals. Nature 476:442–445. https://doi.org/10.1038/nature10291

Lyman, R.L. 2017. Paleoenvironmental reconstruction from faunal remains: ecological basics and analytical assumptions. Journal of Archaeological Research, 25:315–371. https://doi.org/10.1007/s10814-017-9102-6

MacLeod, N. and Rose, K.D. 1993. Inferring locomotor behavior in Paleogene mammals via eigenshape analysis. American Journal of Science 293:300–355. https://doi.org/10.2475/ajs.293.A.300

Martin, T. and Rauhut, O.W.M. 2005. Mandible and dentition of *Asfaltomylos patagonicus* (Australosphenida, Mammalia) and the evolution of tribosphenic teeth. Journal of Vertebrate Paleontology 25:414–425. https://doi.org/10.1671/0272-4634(2005)025[0414:MADOAP]2.0.CO;2

Martin, T. and Koenigswald, W.v. 2020. Mammalian teeth. Form and function. Verlag Dr. Friedrich Pfeil. München.

Mayr, G. 2017. The early Eocene birds of the Messel fossil site: a 48 million-year-old bird community adds a temporal perspective to the evolution of tropical avifaunas. Biological reviews of the Cambridge Philosophical Society 92:1174–1188. https://doi.org/10.1111/brv.12274

Mellett, J.S. 1977. Paleobiology of North American *Hyaenodon* (Mammalia, Creodonta). Contributions to vertebrate evolution, Karger Publishers, Basel.

Mellett, J.S.(1981. Mammalian Carnassial Function and the "Every Effect". In: Journal of Mammalogy 62 (1), S. 164–166. https://doi.org/10.2307/1380488

Merceron, G., Schulz, E., Kordos, L., and Kaiser, T.M. 2007. Paleoenvironment of *Dryopithecus brancoi* at Rudabánya, Hungary: evidence from dental meso- and micro-wear analyses of large vegetarian mammals. Journal of human evolution, 53:331–349. https://doi.org/10.1016/j.jhevol.2007.04.008

Morlo, M. 2004. Diet of *Messelornis* (Aves: Gruiformes), an Eocene bird from Germany. Courier Forschungsinstitut Senckenberg, 252:29–33.

Morlo, M. and Habersetzer, J. 1999. The Hyaenodontidae (Creodonta, Mammalia) from the lower Middle Eocene (MP 11) of Messel (Germany) with special remarks on new x-ray methods. Courier Forschungsinstitut Senckenberg, 216:31–73.

Morlo, M., Gunnell, G.F., and Smith, K.T. 2011. Mammalian carnivores from Messel and a comparison of non-volant predator guilds from the middle Eocene of Europe and North America. 22nd International Senckenberg Conference. Frankfurt am Main, Germany, p. 120.

Mullu, D. and Balakrishnan, M. 2014. Ecology of African Civet *(Civettictis civetta)* in Arba Minch Forest, Arba Minch, Ethiopia. Science, Technology and Arts Research Journal, 3:99–102. https://doi.org/10.4314/star.v3i3.16

Norconk, M.A. 1996. Seasonal Variation in the Diets of White-Faced and Bearded Sakis *(Pithecia pithecia* and *Chiropotes satanas)* in Guri Lake, Venezuela. Norconk, p. 403–423. In Rosenberger, A.L. and Garber, P.A. (eds.), Adaptive Radiations of Neotropical Primates. Springer, Boston, Massachusetts. https://doi.org/10.1007/978-1-4419-8770-9_23

Pemberton, D., Gales, S., Bauer, B., Gales, R., Lazenby, B., and Medlock, K. 2008. The diet of the Tasmanian Devil, *Sarcophilus harrisii*, as determined from analysis of scat and stomach contents. Papers and Proceedings of the Royal Society of Tasmania, 142:13–22. https://doi.org/10.26749/rstpp.142.2.13

Pfaff, C., Nagel, D., Gunnell, G., Weber, G.W., Kriwet, J., Morlo, M., and Bastl, K. 2017. Palaeobiology of *Hyaenodon exiguus* (Hyaenodonta, Mammalia) based on morphometric analysis of the bony labyrinth. Journal of anatomy 230 (2), S. 282–289. DOI: https://doi.org/10.1111/joa.12545

Pineda-Munoz, S., Lazagabaster, I.A., Alroy, J., and Evans, A.R. 2017. Inferring diet from dental morphology in terrestrial mammals. Methods in Ecology and Evolution, 8:481–491. https://doi.org/10.1111/2041-210X.12691

Pollock, T.I., Parrott, M.L., Evans, A.R., and Hocking, D.P. 2021. Wearing the devil down: Rate of tooth wear varies between wild and captive Tasmanian devils. Zoo Biology, 1–14. https://doi.org/10.1002/zoo.21632

Ray, J.C. 1995. *Civettictis civetta*. Mammalian Species, 488:1–7. https://doi.org/10.2307/3504320

Reside, A. and Desantis L.R.G. 2022. Similar forms have similar functions: dental microwear variability in Tasmanian devils, Journal of Mammalogy, 103 (4), S. 891–899. https://doi.org/10.1093/jmammal/gyac042

Rich, T.H.V. 1981. Origin and history of the Erinaceinae and Brachyericinae (Mammalia, Insectivora) in North America. Bulletin of the American Museum of Natural History, 171:1–116.

Rose, R.K., Pemberton, D.A., Mooney, N.J., and Jones, M.E. 2017. *Sarcophilus harrisii* (Dasyuromorphia: Dasyuridae). Mammalian Species, 49:1–17. https://doi.org/10.1093/mspecies/sex001

Rosenberger, A.L. and Kinzey, W.G. 1976. Functional patterns of molar occlusion in platyrrhine primates. American Journal of Physical Anthropology, 45:281–298. https://doi.org/10.1002/ajpa.1330450214

Schultz, J.A. and Martin, T. 2014. Function of pretribosphenic and tribosphenic mammalian molars inferred from 3D animation. Naturwissenschaften, 101:771–781. https://doi.org/10.1007/s00114-014-1214-y

Scott, G.H. 1963. Uniformitarianism, the uniformity of nature, and paleoecology. New Zealand Journal of Geology and Geophysics, 6:510–527. https://doi.org/10.1080/00288306.1963.10420063

Shippley, S.J., Manning, A.D., Wilson, B.A., Newport, J., Neeman, T., Gordon, I.J., and Neaves, L.E. 2025. Trophic rewilding: The diet of an opportunistic mesopredator. Biological Conservation, 302. https://doi.org/10.1016/j.biocon.2025.111004

Simpson, G.G. 1936. Studies of the earliest mammalian dentitions. Dental Cosmos, 78:791–800.

Smith, K.T., Schaal, S.F.K., and Habersetzer, J. 2018. Messel – An ancient Greenhouse Ecosystem, E. Schweizerbartsche Verlagsbuchhandlung, Stuttgart.

Smith, K.T., Collinson, M., Folie, A., Habersetzer, J., Hennicke, F., Kothe, K., Lehmann, T., Lenz, O.K., Mayr, G., Micklich, N., Rabenstein, R., Racicot, R., Schaal, S.F.K., Smith, T., Tosal, A., Uhl, D., Wappler, T., Wedmann, S., and Wuttke M. 2024. The biodiversity of the Eocene Messel Pit. Palaeobiodiversity and Palaeoenvironments, 104:859–940 https://doi.org/10.1007/s12549-024-00633-2

Solé, F. and Ladevèze, S. 2017. Evolution of the hypercarnivorous dentition in mammals (Metatheria, Eutheria) and its bearing on the development of tribosphenic molars. Evolution & Development, 19: 56–68. https://doi.org/10.1111/ede.12219

Solé, F. and Mennecart, B. 2019. A large hyaenodont from the Lutetian of Switzerland expands the body mass range of the European mammalian predators during the Eocene. Acta Palaeontologica Polonica, 64:275–290. https://doi.org/10.4202/app.00581.2018

Solé, F., Morlo, M., Schaal, T., and Lehmann, T. 2021. New hyaenodonts (Mammalia) from the late Ypresian locality of Prémontré (France) support a radiation of the hyaenodonts in Europe already at the end of the early Eocene. Geobios, 66-67:119–141. https://doi.org/10.1016/j.geobios.2021.02.004

Stannard, H.J., Tong, L., Shaw, M., Sluys, M.v., McAllan, B., and Raubenheimer, D. 2017. Nutritional status and functional digestive histology of the carnivorous Tasmanian devil *(Sarcophilus harrisii).* Comparative biochemistry and physiology Part A: Molecular & integrative physiology, 205:1–7. https://doi.org/10.1016/j.cbpa.2016.12.008

Stover, K.K. and Williams, S.H. 2011. Intraspecific scaling of chewing cycle duration in three species of domestic ungulates. The Journal of experimental biology, 214:104–112. https://doi.org/10.1242/jeb.043646

Strait, S.G. 1993. Molar Morphology and Food Texture among Small-Bodied Insectivorous Mammals. Journal of Mammalogy, 74:391–402. https://doi.org/10.2307/1382395

Tamagnini, D., Meloro, C., Raia, P., and Maiorano, L. 2021. Testing the occurrence of convergence in the craniomandibular shape evolution of living carnivorans. Evolution; international journal of organic evolution, 75:1738–1752. https://doi.org/10.1111/evo.14229

Tiffney, B.H. 2008. Phylogeography, Fossils, and Northern Hemisphere Biogeography: The Role of Physiological Uniformitarianism. Annals of the Missouri Botanical Garden, 95:135–143. https://doi.org/10.3417/2006199

Tütken, T. 2014. Isotope compositions (C, O, Sr, Nd) of vertebrate fossils from the Middle Eocene oil shale of Messel, Germany: Implications for their taphonomy and palaeoenvironment. Palaeogeography, Palaeoclimatology, Palaeoecology, 416:92–109. https://doi.org/10.1016/j.palaeo.2014.08.005

Ungar, P.S. 2010. Mammal teeth. Origin, evolution, and diversity. Johns Hopkins University Press, Baltimore, Maryland. https://doi.org/10.1353/book.485

Valkenburgh, B.v. 1988. Trophic Diversity in Past and Present Guilds of Large Predatory Mammals. Paleobiology, 14:155–173 https://doi.org/10.1017/S0094837300011891

Valkenburgh, B.v. 1999. Major Patterns in the History of carnivorous Mammals. Annual Review of Earth and Planetary Sciences, 27:463–493 https://doi.org/10.1146/annurev.earth.27.1.463

Valkenburgh, B.v. 2007. *Déjà vu*: the evolution of feeding morphologies in the Carnivora, Integrative and Comparative Biology, 47:147–163. https://doi.org/10.1093/icb/icm016

Wall, C.E., Vinyard, C.J., Johnson, K.R., Williams, S.H., and Hylander, W.L. 2006. Phase II jaw movements and masseter muscle activity during chewing in *Papio anubis*. American Journal of Physical Anthropology, 129:215–224. https://doi.org/10.1002/ajpa.20290

Warburton, N.M., Withers, P.C., and Martin, M. 2024. More than one way to eat a mouse: Skull shape variation within a monophyletic group of mammals (Marsupialia; Dasyurinae). Journal of Zoology, 322:76–88. https://doi.org/10.1111/jzo.13124

Werdelin, L. 1987. Jaw geometry and molar morphology in marsupial carnivores: analysis of a constraint and its macroevolutionary consequences. Paleobiology, 13:342–350. https://doi.org/10.1017/S0094837300008915

Witmer, L.M. and Rose, K.D. 1991. Biomechanics of the Jaw Apparatus of the Gigantic Eocene Bird *Diatryma:* Implications for Diet and Mode of Life. Paleobiology, 17:95–120. https://doi.org/10.1017/S0094837300010435

Zack S.P. 2019a. The first North American *Propterodon* (Hyaenodonta: Hyaenodontidae), a new species from the late Uintan of Utah. PeerJ. 7:e8136 https://doi.org/10.7717/peerj.8136

Zack, S. P. 2019b. A skeleton of a Uintan machaeroidine ‘creodont’ and the phylogeny of carnivorous eutherian mammals. Journal of Systematic Palaeontology 17:653–689. https://doi.org/10.1080/14772019.2018.1466374

APPENDIX 1.

Chewing cycle of *Lesmesodon edingeri* reconstructed in the OFA. Collisions detected by the program are shown in colored areas. Reconstructed chewing cycle followed by the lower molars is shown as orange line. Not to scale.

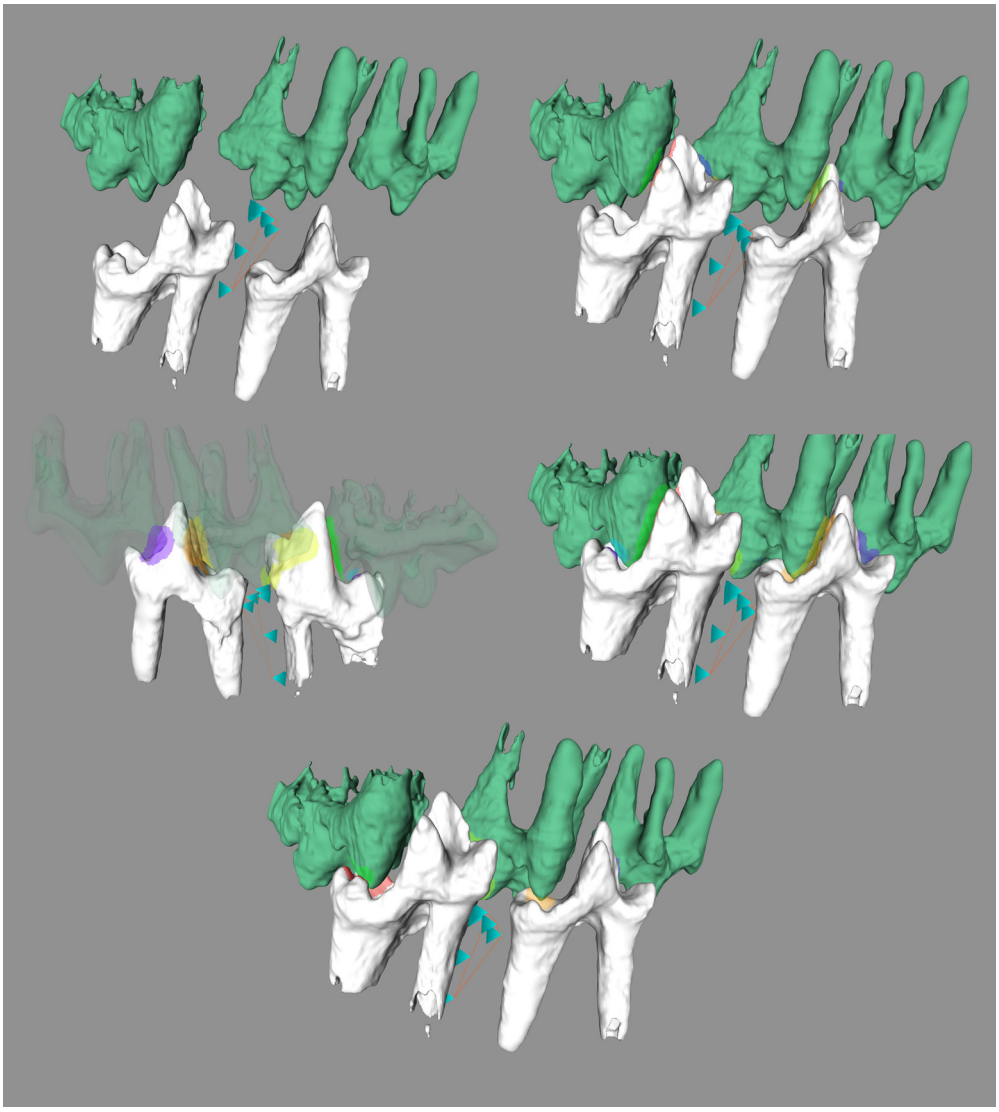

APPENDIX 2.

Chewing cycle of *Proviverra typica* reconstructed in the OFA. Collisions detected by the program are shown in colored areas. Reconstructed chewing cycle followed by the lower molars is shown as orange line. Not to scale.

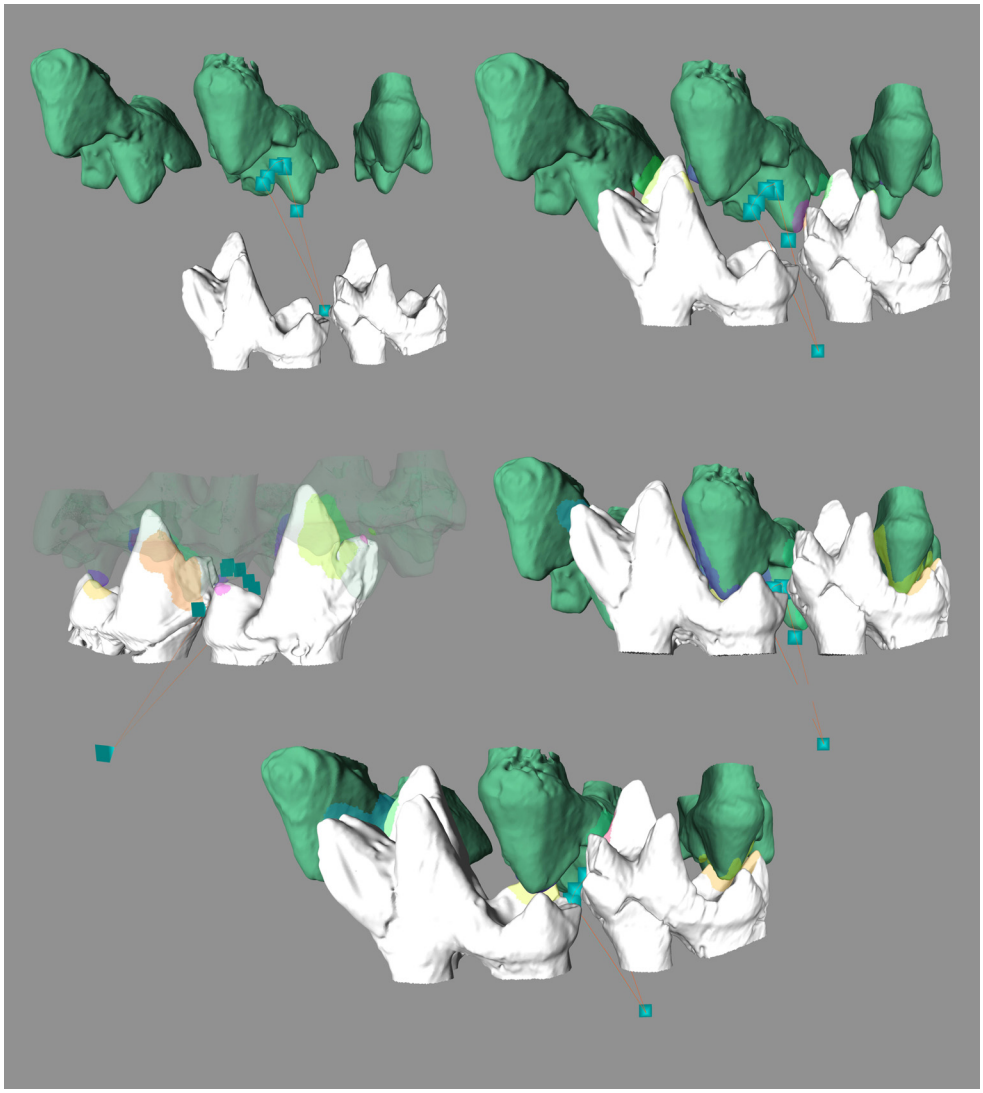

APPENDIX 3.

Chewing cycle of *Dasyurus viverrinus* reconstructed in the OFA. Collisions detected by the program are shown in colored areas. Reconstructed chewing cycle followed by the lower molars is shown as orange line. Not to scale.

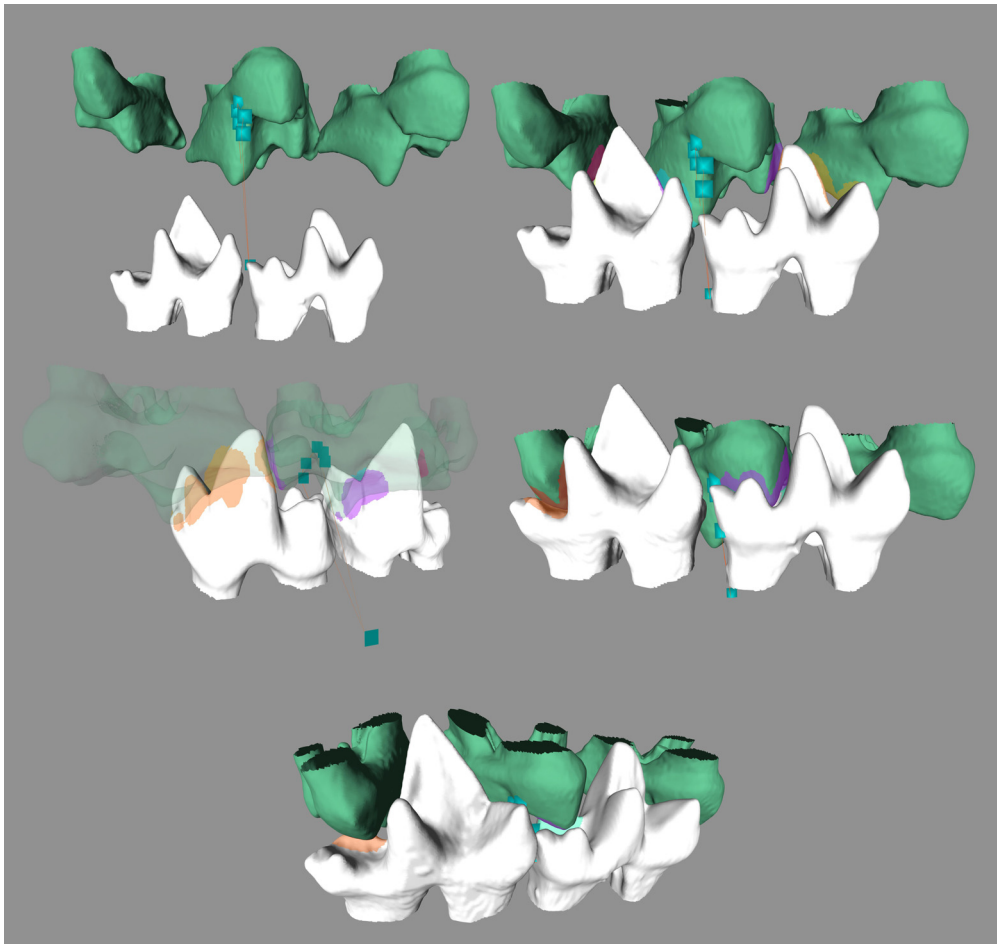

APPENDIX 4.

Chewing cycle of *Sarcophilus harrisii* reconstructed in the OFA. Collisions detected by the program are shown in colored areas. Reconstructed chewing cycle followed by the lower molars is shown as orange line. Not to scale.

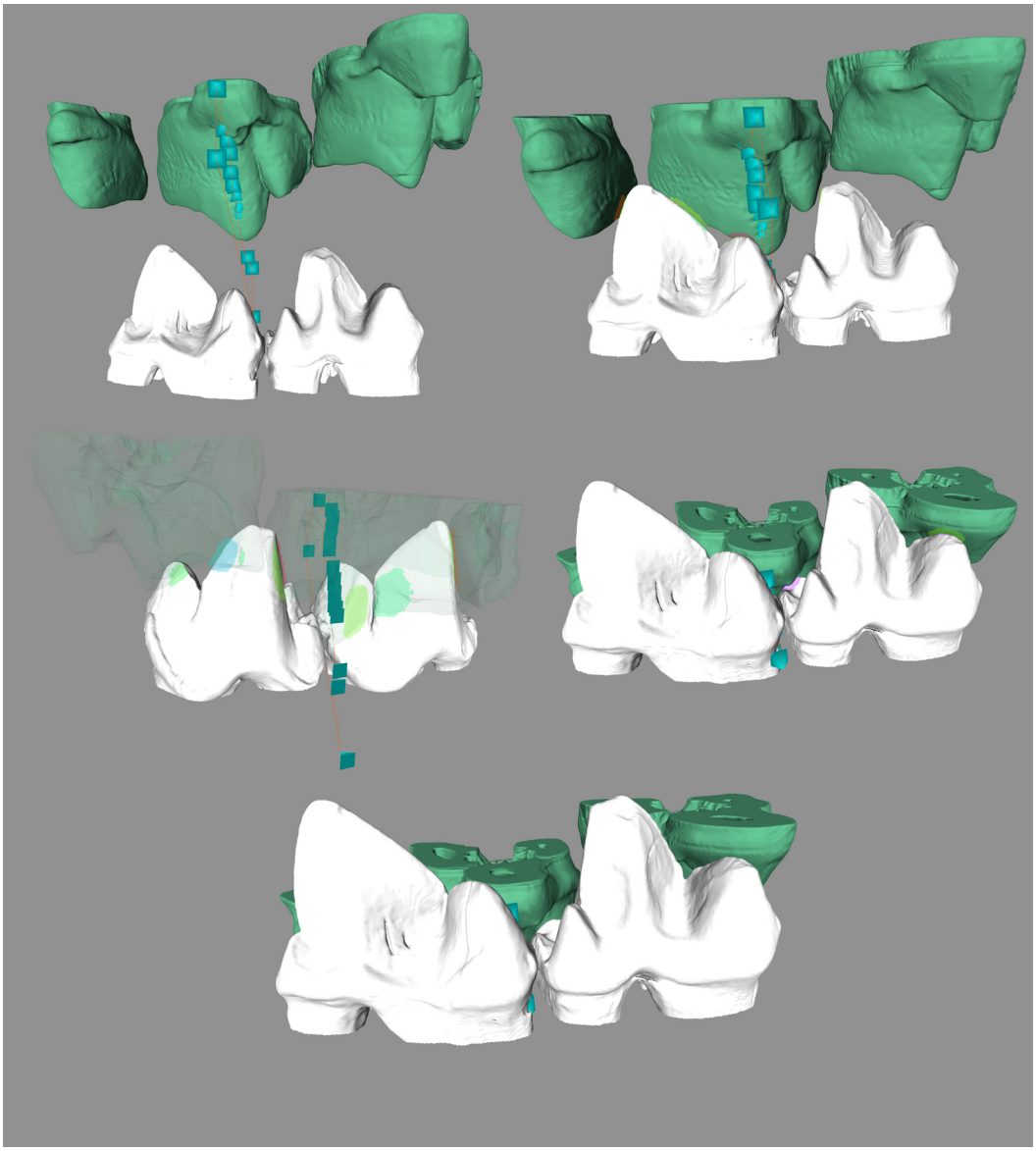

APPENDIX 5.

Chewing cycle of *Civettictis civetta* reconstructed in the OFA. Collisions detected by the program are shown in colored areas. Reconstructed chewing cycle followed by the lower molars is shown as orange line. Not to scale.